EMERGENCY MANAGEMENT (MITIGATION, PREPAREDNESS, AND RAPID RESPONSE) OF LANDSLIDE DAM HAZARDS – A REVIEW

JIA-JYUN DONG[1]

[1] *Graduate Institute of Applied Geology, National Central University, Taiwan, jjdong@geo.ncu.edu.tw*

Introduction

Outburst flood from landslide barrier lakes is hazardous to the downstream of the nature dams. Inundation upstream of the landslide dams induced casualties and properties loss as well. Since the landslide dams are usually short-lived, emergency management is challenge because rapid responses are required. Costa (1985) published one USGS report "Floods from dam failures" (include landslide dams and constructed dams) in 1985. This is an important documentation from the hazard assessment view point of landslide dam hazards. The special publication of ASCE "Landslide Dams: Processes, Risk, and Mitigation" (Schuster, 1986), consisted of nine papers on landslide dams, could be one of the pioneer collections for landslide dam study. The landslide processes involved in forming landslide dams, the potential for catastrophic failure of the dams, and upstream/downstream effects of the dams are introduced. Case histories from the United States, Canada, Pakistan, Japan, and China are illustrated. Two years later, Costa and Schuster (1988) published a classical review paper of "The formation and failure of natural dams" (related to landslides, glacial-ice, and moraine), which using "an integrated view of the phenomenon as a whole". Soon after this review, Costa and Schuster (1991) documented 463 historical landslide dam cases from all around the world. This documentation is the most important landslide dam inventory in 90's. In 2002, Korup (2002) published an important review paper on geomorphic and hydrologic aspects of the formation, failure and geomorphic impact of landslide dams. Although this is a very comprehensive review of landslide dam study, the conclusions of this paper pointed out that there is a considerable lack of understanding of geomorphic forms and processes involved with landslide-dam formation, stability and failure.

For the past two decades, together with the increasingly understanding of landslide dam evolution, the technologies acquiring critical information for landslide dam hazard mitigation have been significantly improved. Many comprehensive books and review papers (e.g., Evans et al., 2011; Zhang et al., 2016; Zheng et al., 2021; Zhong et al., 2021; Fan et al., 2020; 2021) were published, based on the new database, numerical and experimental tests, and case histories of landslide dams. Worldwide landslide dam inventories are accumulated continuously as well. However, few review comprehensively gathering knowledge relevant to emergency management. Thorough reviews focusing on available technologies for emergency management is needed.

Methods

In this study, state of the art review focuses on the issues which are relevant to emergency management (McLoughlin, 1985) of possible short-live landslide dams including: predicting river blockage and providing scenarios (preparedness before the dam forming), early identifying the dam forming (secure more time for emergency response), rapidly evaluating the hazards (risk) of landslide dam (upstream and downstream), and short-term measures (hard and soft ones) to mitigate the hazards.

Results

Emergency management strategies before the landslide dam forming (preparedness) are illustrated, including (a) data collection (including landslide dam inventory), (b) susceptibility analysis, and (c) possible hazard scenarios development. Moreover, technologies for early identifying the occurrence, location, and characteristics of landslide dam and related lake are introduced, including (a) landquake, (b) abnormal hydrogeological response, and (c) remote sending data. Relevant information required for emergency management is indicated, too. Finally, rapid hazard evaluation methods are summarized, including (a) downstream (stability, breach process, and flood routing), and (b) upstream (predicting the temporal variation of lake surface elevation). Thanks to the quick development of new technologies, preparedness and rapid assessment of the landslide dam hazards soon after the formation of a landslide dam is possible for decision-making to prevent or minimize the losses.

Conclusion

The author reviewed many review papers, books, and documentations and surprisingly found out few of them focused on comprehensively gathering knowledge relevant to emergency management. This review will be a useful reference for emergency management of landslide dam hazards.

References

Costa, J. E. Floods from Dam Failures, Open-File Report 85-560, US Geological Survey. 1985.

Costa, J.E.; Schuster, R.L. The formation and failure of natural dams. *Geol. Soc. Am. Bull.* 1988, 100 (7), 1054 – 1068.

Costa, J. E.; Schuster, R. L. Documented Historical Landslide Dams from around the World, Open-File Report 91-239, US Geological Survey. 1991.

Evans, S. G. The maximum discharge of outburst floods caused by the breaching of man-made and natural dams. *Canadian Geotechnical Journal*, 1986, 23(3), 385-387.

Evans, S. G.; Hermanns, R. L.; Strom, A.; Scarascia-Mugnozza, G. (eds.). Natural and artificial rockslide dams (Vol. 133). Springer Science & Business Media. 2011.

Fan, X.; Dufresne, A.; Subramanian, S. S.; Strom, A.; Hermanns, R.; Stefanelli, C. T.; Hewitt, K.; Yunus, A.P.; Dunning, S.; Capra, L.; Geertsema, M.; Miller, B.; Casagli, N; Jansen, J.D.; Xu, Q. The formation and impact of landslide dams–State of the art. *Earth-Science Reviews*, 2020, 203, 103116.

Fan, X.; Dufresne, A.; Whiteley, J.; Yunus, A. P.; Subramanian, S. S.; Okeke, C.A.U.; Panek., T.; Hermanns., R.L.; Peng, M.; Strom, A.; Havenith, H.B.; Dunning, S.; Wang, G.; Stefanelli, C. T.. Recent technological and methodological advances for the investigation of landslide dams. *Earth-Science Reviews*, 2021, 218, 103646.

Korup, O. Recent research on landslide dams-a literature review with special attention to New Zealand. *Progress in Physical Geography*, 2002, 26(2), 206-235.

McLoughlin, D. A framework for integrated emergency management. *Public administration review*, 1985, 45, 165-172.

Zhang, L.M.; Peng, M.; Chang, D.S.; Xu, Y. Dam Failure Mechanisms and Risk Assessment. John Wiley & Sons Singapore Pte. Ltd., Singapore. 2016.

Zheng, H.; Shi, Z.; Shen D, Peng, M.; Hanley, K.J.; Ma, C.; Zhang, L. Recent Advances in Stability and Failure Mechanisms of Landslide Dams. *Front. Earth Sci.,* 2021, 9:659935. doi: 10.3389/feart.2021.659935

Zhong, Q.; Wang, L.; Chen, S.; Chen, Z.; Shan, Y.; Zhang, Q.; Ren, Q.; Mei, S.; Jiang, J.; Hu, L.; Liu, J. Breaches of embankment and landslide dams-State of the art review. *Earth-Science Reviews*, 2021, 216, 103597.

EVALUATION OF FAILURE TYPES AND EVOLUTION OF A DEEP-SEATED LANDSLIDE, TAICHUNG CITY, TAIWAN

ABSTRACT

CHE-MING YANG [1], CHIA-LUNG HSIEH [1]

[1] *Department of Civil and Disaster Prevention Engineering, National United University, Taiwan, stanleyyangcm@nuu.edu.tw*

Introduction

Deep-seated landslides typically exhibit complex failure patterns due to their considerable depth, area, and volume, often triggered by intense rainfall and seismic activity. The response of such landslides varies depending on the triggering and types of failure involved. The geological and geomorphological context plays a crucial role in the types of rock slope failures, particularly influenced by the orientations of discontinuities and slope surfaces (Korup et al., 2010). Rock slope failures can be classified into planar sliding, wedge sliding, toppling, and rockfall (Stead and Wolter, 2015), with some landslides showing a combination of two or more failure types. The distinct rock slope failure mechanisms result in different kinematic processes and consequences, affecting disaster prevention and mitigation strategies. Therefore, a comprehensive assessment of failure types and their magnitudes is essential for effective disaster. This study focuses on deep-seated landslide (4 ha in area, ~14.5m in depth) in Taichung City, central Taiwan with the aim of establishing its geological model. The landslide occurs within a flysch foreland sequence of the Miocene Cholan Formation, adjacent to the of wall the Chelungpu Fault. The cuesta landform predominant prevalent in this region.

Methods

Based on the regional geological map, high-resolution digital elevation model, digital surface model, and multi-period images, this study employs various methodologies: (a) field investigation involving analysis of discontinuity attitudes and observation of outcrops; (b) geomorphological analysis including topographic interpretation and slip surface trace; (c) geotechnical exploration through boreholes and underground monitoring; (d) orthoimage interpretation incorporating the landslide's failure history. As a result, this comprehensive approach enables the establishment of a geological model and evolution of a deep-seated landslide (Fig. 1).

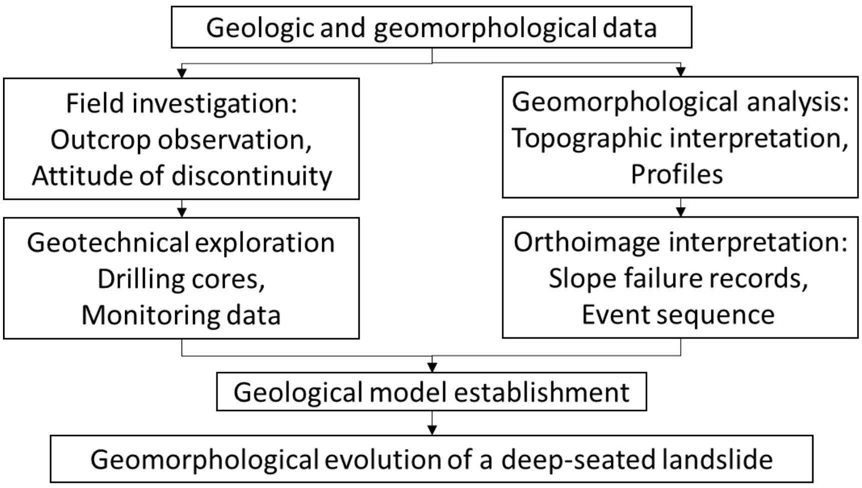

Figure 1. *Flowchart of this study.*

Results

The field investigation revealed the potential slip zone surrounding the landslide site, with a survey conducted on adjacent outcrops to analyze the lithology and attitudes of bedding planes and joint sets. The topographic features of landslide were identified, and the main scarp and right limb cliff corresponding to distinct two joint sets. Analysis of multi-temporal orthoimages depicting the slope failure indicated the extent and locations of past failures, providing insights into the sequence of events and the relationships between different sections within the deep-seated landslide. However, orthoimages were found to be insufficient in identifying variations in the right limb cliff. Therefore, a combination of field surveys and aerial views obtained through the use of drones is deemed essential for this study. A 3D model was constructed to visualize and present the spatial information of the deep-seated landslide. The failure mechanisms were categorized into four types: (1) rockfalls occurring at the main scarp and the right limb cliff, (2) planar sliding along the bedding of the upper slope, (3) wedge failure at the intersection of the main scarp and right limb cliff and, (4) colluvium circular failure in the lower slope. Based on the findings of investigation, it is observed that planar sliding along the bedding plane near the riverside is likely to initiate at the initial stages, leading to the elevation difference at the right limb, resulting in the formation of a high cliff. Over the long term, the uplift of the Chelungpu thrust fault has reduced the stability of inclined sedimentary rocks, causing the enlargement and thickening of the daylighted rock layers. The slope failures develope from the lower slope to the upper slope, the main scarp develops backward progressively due to planar failure. Additionally, rockfall events are noted to occur along the main scarp. Furthermore, the bedding plane dips to southeast and the right limb cliff faces to north with east-west strike. The intersection of two discontinuities form the wedges plunging to the east. The deposits of three failure zones mentioned above moves downslope, resulting in the accumulation of a thick colluvium.

Moreover, the deposits increase the loading and the toe erosion both worsen the stability of colluvium. The significant displacement of colluvium was identified by orthoimages, which induced by heavy rainfall. After colluvium descends, the daylighted rock layers and wedges on the upper slope become prone to instability. Consequently, dynamic interaction is likely to persist over the long term.

Conclusion

A geological model of deep-seated landslide has been developed, identifying four distinct failure types (rockfalls, planar failure, circular failure, and wedge failure) by field survey, analysis, and interpretation of orthoimages. Furthermore, the geomorphologic evolution of a deep-seated landslide can be clarified by examining the interplay of these four types of failure.

Acknowledgements

This research was supported by the National Science and Technology Council (NSTC- 112-2116-M-239-001) and National United University (project No. SM113004).

References

Korup, O.; Densmore, A. L.; Schlunegger, F. The role of landslides in mountain range evolution. *Geomorphology*. 2010, 120(1-2), 77-90.

Stead, D.; Wolter, A. A critical review of rock slope failure mechanisms: The importance of structural geology. *Journal of Structural Geology*. 2015, 74, 1-23.

ROTENFELS: ANALYSIS OF THE ROCKFALL HAZARD ON THE HIGHEST ROCK FACE NORTH OF THE ALPS

STEVE GRUSLIN [1], TIFFANY HENNEBAUT [2], ANAÏS ENDRÈS [3]

[1] *GEOCONSEILS, Luxembourg, steve.gruslin@geoconseils.lu*

[2] *GEOCONSEILS, Luxembourg, tiffany.hennebaut@geoconseils.lu*

[3] *ECOLE NATIONALE SUPERIEURE DE GEOLOGIE, France, anais.endres1@etu.univ-lorraine.fr*

Introduction

The Rotenfels rhyolitic rock face in Bad Münster am Stein-Ebernburg (Germany), the highest north of the Alps (over 200m high), presents a particular risk of falling and scattered boulders. In recent years, numerous blocks have fallen onto the road and railway below. Protection against geological hazards is complicated by the fact that the site is a protected natural area. It is therefore impossible to secure the rock face directly, and boulder barriers are the only possible solution. Boulder barriers already exist in various places, but they are currently insufficient to protect the road and railway effectively. The study we carried out had several objectives: identify the geological risks that could affect the road and railway, determine, where there is no fence, the rebound energies and heights that the fences to be installed will have to absorb, and, where there are already fences, to establish whether the current fences are suitable and which part requires additional fences. The safety measures to be implemented were determined by means of an in situ characterisation of the rock, a risk analysis and trajectometric studies.

Figure 1. Two views of Rotenfels, with the road and railway line to be protected clearly visible

Methodology

Based on field observations, the entire site was divided into 19 zones with similar characteristics in terms of topography, wall height, rock aspect, ground occupation at the foot of the wall, etc. For each of the zones thus defined, except few zones that were not accessible, the rock was characterised by a series of in situ measurements including stereographic measurements, a survey of the instabilities affecting the wall, Rockschmidt hammer measurements and a classification of the rock mass according to several internationally recognised systems (Q, RMR, GSI). All the measurements taken in the field were used for our risk analysis, enabling us to define the areas from which the blocks could have originated and the dimensions of the unstable boulders to be expected. The size of the critical blocks (plurimetric), and the blocks found on the ground (around $0.1m^3$), have been added to estimate a volume of blocks (between $0.1m^3$ and $1m^3$) that should be modelised in the trajectory modelisations. Small stones ($<0.1m^3$) have also been modelised, according to the volume of scree cone found on site.

Trajectometric study and rocfall simulations

Three main types of blocks have been defined. The volume of the blocks was defined by field

assessment, i.e.: the critical volume of the block verified for each zone, the orientation of the various joints and their persistence, and the volume of the block found on the ground or at the foot of the slope for each zone. These observations enable us to estimate two main scales of boulder, with a volume of around 0.1 – 0.2m^3, and a volume of around 1m^3. The small rocks (from 0.0005m^3 to 0.1m^3) have also been modelised by the interpretation of scree cone volume. The distribution has been changed in function of the zone classification: the most fractured areas present more 0.1m^3 blocks, and the more massive areas 0.2m^3 blocks. To a lesser extent, boulders with a volume of 5m^3 were also modelled to consider the collapse of the largest elements. This volume of 5m^3 is an average volume given the fragmentation of the block along the fall and the rebound. Some exceptional boulders, close to the foot of the cliff, have been modelled with a volume of 10m^3. But these events remain exceptional, and therefore have not been used to estimate the energy and rebound to be taken up by the barriers.
The 2D simulations with large boulders were made only for critical cuts or where large blocks were suspected on site. For the 3D simulations, the contour lines acquired by Lidar were imported and all the observations collected in the field were uploaded to the 3D model (weathered areas, critical blocks, scree cone, angle slope …). The 3D representation was used to model the propagation of the blocks in space. It also allowed to represent the ended point of each modelised block. The parameters used in the simulations were based on the Schmidt hammer when measurement have been possible (Rayudu, 1997), or from the Rocfall library.

Results

The simulations show that the ended point could reach the road and the train tracks. Thanks to these simulations, we have been able to converge the models results with the observations made on site. We were thus able to estimate the propagation hazard, which will draw the areas to be treated as a priority. Thanks to the 3D refined model, we were also able to precise the most critical areas where the fences should be installed or renewed. These results are limited to blocks with a 95% probability of occurrence, which means that the more extreme results (i.e. exceptional block size) are considered exceptional events with an acceptable occurrence rate for users.

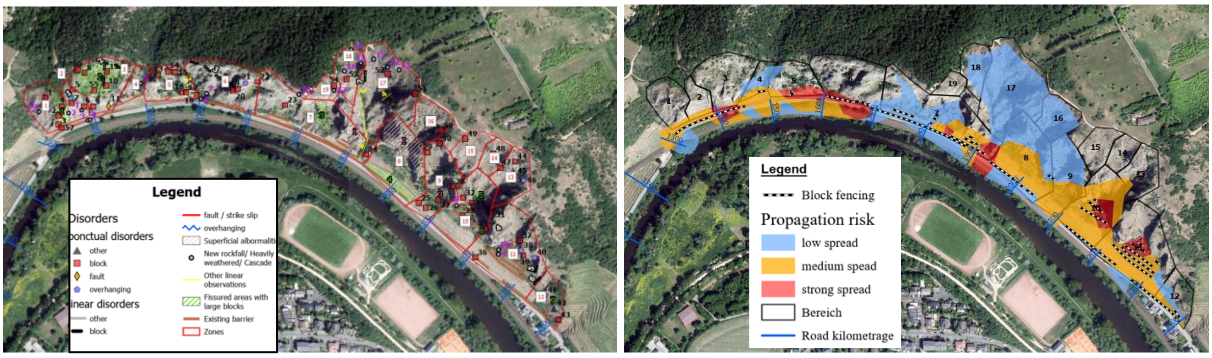

Figure 2. Zoning of the site studied into 19 zones with the diverse observations made on site (left**)** and map of the propagation hazard (right)

Conclusion

All the calculations have shown that the risk is very real for road and railway. The methodology put in place, enabling the acquisition of the field data's needed for the trajectometric calculations, made it possible to determine the input data's (energy and height of rebound) needed to dimension, in a second phase, the safety measures to be implemented to protect the road and the railway line.

References

Landsamt für Geologie und Bergbau Rheinland-Pfalz, *Geologie von Rheinland-Pfalz,* Stuttgart, E. Schweizerbart'sche Verlagsbuchhandlung (Nägele u. Obermillen), 2005.

Rayudu DNP, *Computer simulations of rockfalls – Application to rockfalls at fox glacier, West Coast, New Zealand*, Thesis, Lincoln University, 1997.

LARGE-SCALE LANDSLIDE SUSCEPTIBILITY ZONATION: CLASSIFICATION METHODS AND INFLUENCE ON A FURTHER APPLICATION IN SPATIAL PLANNING SYSTEM

SANJA BERNAT GAZIBARA [1], IVA ŠTEFIČAR [1], MARKO SINČIĆ [1], MARTIN KRKAČ [1], SNJEŽANA MIHALIĆ ARBANAS [1]

[1] *University of Zagreb, Faculty of Mining, Geology and Petroleum Engineering, Croatia, sanja.bernat@rgn.unizg.hr*

Introduction

Classification of landslide susceptibility maps (LSMs) is crucial for land use spatial planning and management, and it affects the possibilities of practical use of maps and the quality of information depicted by the map. Adopting one classification system or another will affect the map's readability, final appearance, and, most importantly, the decision-making tasks required for effective land management. This research compares and evaluates the reliability of the most commonly used classification methods and proposes a classification based on the Receiver Operating Characteristic (ROC) curve. The analyses were carried out on the landslide susceptibility model for the study area (20 km^2) in Hrvatsko zagorje (Croatia), which was derived in the frame of the LandSlidePlan project (Bernat Gazibara et al., 2022).

Methods

The landslide susceptibility model for the study area in Hrvatsko zagorje was derived from a detailed LiDAR-based landslide inventory (Krkač et al., 2022), high-resolution geoenvironmental causal factors and by applying the Random Forests method. Stable pixels were randomly generated in the same quantity as unstable pixels, outside the known landslide areas identified in the LiDAR-based inventory. For landslide susceptibility modelling, 50% of the landslide polygons in the inventory were randomly selected for the model training and the remaining 50% for model validation, while 100% of the mapped landslides were used for susceptibility zoning. Considering landslide causal factors, a set of eight maps grouped as geomorphological (slope, aspect, curvature), geological (engineering formations, proximity to engineering formations), hydrological (proximity to drainage network, proximity to permanent streams) and anthropogenic (proximity to land-use contact) were prepared from LiDAR DTM 5m resolution, engineering geological map in scale 1:5000 (Sinčić et al., 2022), and existing high-resolution land use data. The derived landslide susceptibility model showed high model verification AUC (85.1 %) and can be considered representative for further analysis. The classification methods used in this analysis were equal intervals, quantiles, natural breaks, geometrical intervals, standard deviation and classification based on the ROC curve expressed by cumulative landslide area and cumulative landslide susceptibility, i.e. probability. Furthermore, cut-off values for zonation using the ROC curve were set to different cumulative landslide area presence. Derived LSMs were classified into five zones: very low, low, medium, high and very high susceptibility zones.

Results

To analyse the influence of eight classification methods on landslide susceptibility zoning, the percentage of susceptibility zones in the study area and the percentage of landslide presence in each susceptibility zone were calculated (Figure 1). The criteria for choosing the optimal method is that the zonation results in a map with a low percentage of high and very high susceptibility zones containing a high landslide presence. On the contrary, low and very low susceptibility zones should contain low landslide presence. Considering the above, the method based on the ROC curve with different threshold values proved to be the most optimal method for landslide susceptibility zonation in the study area. The methods of equal intervals, natural breaks, and standard deviations resulted in LSMs with a low percentage of the study area in very high susceptibility zones with low landslide presence. The quantile method and geometrical intervals resulted in a lower percentage of the study area in very low susceptibility zones compared to the LSMs classified based on the ROC curve.

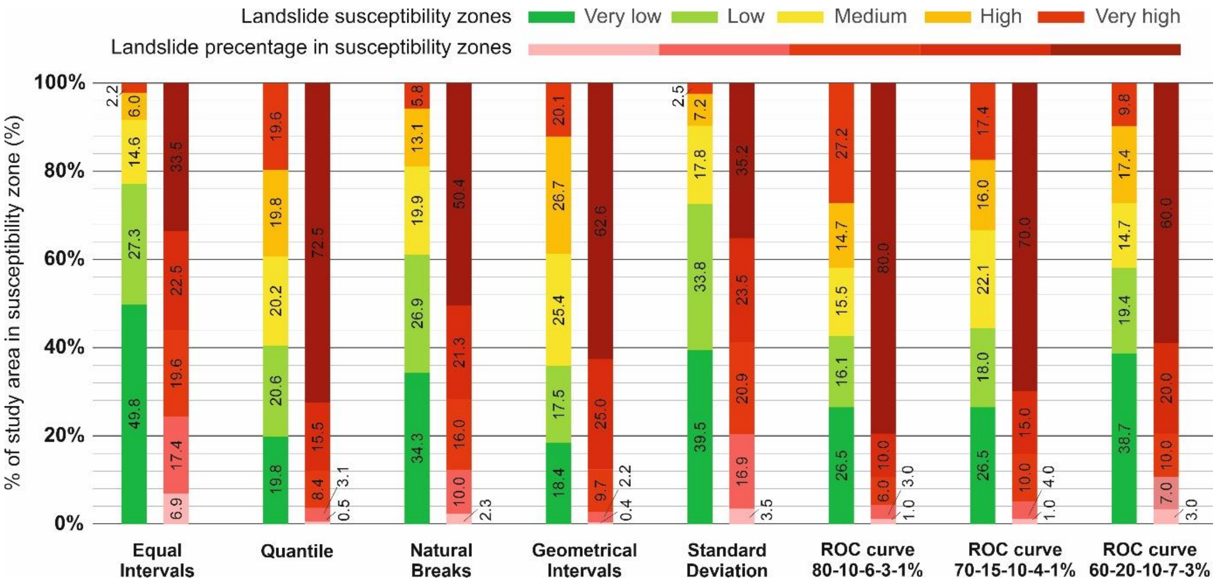

Figure 1. Distribution of landslide susceptibility zone areas and landslide presence based on eight different classification methods.

Conclusion

Derived landslide susceptibility zonation maps differ based on the area of susceptibility zones and the percentage of known landslides in susceptibility zones. Since the most effective and generally cheapest risk mitigation measures are non-structural measures based on land use planning, these large differences in the interpretation of landslide susceptibility zones can impact responsible and sustainable spatial planning and risk assessment at a local level. We conclude that landslide susceptibility zonation by applying the ROC curve enables the interpretation of smaller areas of high and very high susceptibility zones with high landslide presence; the only precondition is that landslide susceptibility modelling is based on representative and reliable LiDAR-based inventory.

References

Bernat Gazibara, S.; Mihalić Arbanas, S.; Sinčić, M.; Krkač, M.; Lukačić, H.; Jagodnik, P.; Arbanas, Ž. LandSlidePlan -Scientific Research Project on Landslide Susceptibility Assessment in Large Scale. *In Proceedings of the 5th ReSyLAB*, Rijeka, Croatia, 23-26 March 2022; pp. 99–106.

Krkač, M.; Bernat Gazibara, S.; Sinčić, M.; Lukačić, H.; Mihalić Arbanas, S. Landslide Inventory Mapping Based on LiDAR Data: A Case Study from Hrvatsko Zagorje (Croatia) *In Proceedings of the 5th ReSyLAB*, Rijeka, Croatia, 23-26 March, 2022; pp. 81–86.

Sinčić, M.; Bernat Gazibara, S.; Krkač, M.; Lukačić, H.; Mihalić Arbanas, S. The Use of High-Resolution Remote Sensing Data in Preparation of Input Data for Large-Scale Landslide Hazard Assessments. *Land*. 2022, 11, 1360, doi:10.3390/land11081360.

REMEDIATION WORKS ON AN ACTIVE LANDSLIDE IN SVÄTÝ ANTON, SLOVAKIA

MARTIN BEDNARIK[1], RÓBERT CSIZMADIA[2], RENÉ PUTIŠKA[1], BIBIANA BRIXOVÁ[1], RUDOLF TORNYAI[1] & ALEŠ HAVLÍN[3]

[1]*Comenius University Bratislava, Faculty of Natural Sciences, Department of Engineering Geology, Hydrogeology and Applied Geophysics, Slovakia; mbednarik@uniba.sk*

[2]*GEOFOS, Ltd., Žilina, Slovakia,* robert.csizmadia@geofos.sk

[3]*National Radiation Protection Institute, Brno, Czech Republic*

Introduction

Due to the increasing activity of slope movements, an emergency was declared in the village of Svätý Anton on February 8, 2021. The landslide in Svätý Anton posed an immediate risk to the main road no. I/51, its traffic, and the surrounding infrastructure. The landslide in Svätý Anton represents a reactivated form of an old landslide. The condition for its creation in the past was a favorable geological structure; Neogene fine-grained and sandy tuffs, which, due to weathering processes, acquired the character of fine-grained soils with unfavorable physical and mechanical properties and erosive activity of the Štiavnica stream. The current activity state is caused by anomalous precipitation in this environment.

Methods

In the first phase, comprehensive drainage of the landslide area was proposed and implemented, both surface and deep drainage. The second phase addressed permanent stabilization measures to secure the toe of the landslide slope along the road by constructing a retaining wall to achieve local stability on the specific shear surface and to ensure the required passable width of the first-class communication 1/51 and its drainage, which was non-functional before the commencement of the works. The rescue works in the second phase were designed as a two-stage steel anchored construction. A flexible, stabilizing, and simultaneously permeable construction was proposed. Both stages of security are formed from an anchored steel stabilization structure. The approach to the design of the second phase was initiated after analyzing the stability situation of the massif post-drainage and evaluating the effectiveness of the constructed drainage elements. The evaluation also included the results of measurements from geotechnical monitoring and geophysical measurements. The existing monitoring network was expanded as part of the rescue works.

Results

A surface drainage system was implemented to reduce the contribution of precipitation to the body of the landslide. To lower the level of the groundwater level, subhorizontal drainage wells and prefabricated drainage drains were designed and implemented at the foot of the slope deformation. ZUBOR prefabricated drainage geodrains (Fig. 1 left) were realized in the foot of the landslide body at an axial distance of 1.50 m with a slope of 3°. They were installed in the rock environment using mechanical vibration equipment. Horizontal drainage wells (Fig. 1 middle) were realized with a drilling rig using coreless technology with a full profile lost rolling chisel. The initial approx. 20 m was realized with a drilling diameter of Ø 156 mm, while the pipes were not perforated (wells below the road). The remaining length of the wells was perforated, min. 5% of the casing area (pipe diameter 89 mm). The outlet of the wells is in a low concrete wall, while the water is drained directly into the recipient - Štiavnica stream. Drainage branches 1 and 2 are located on the sides of the landslide body and branch off in the crown of the landslide, they are designed for the most efficient capture of water above the landslide body (Fig. 1 right). A control shaft is located on each drainage branch, used for the capture and sedimentation of fine-grained material in sludge pits, and for visual monitoring of the functionality of the system. As part of the first stage of immediate emergency measures, reconstruction works were also carried out - cleaning and modification of the outlet part of the culvert into the recipient of the Štiavnica stream, cleaning of the existing culvert under the road, repair of the inflow part of the culvert and reconstruction of the road ditch. The retaining wall was designed as a two-stage steel anchored structure (Fig. 2 left). A flexible, stabilizing and at the same time permeable structure was designed, which does not prevent the drainage of the accumulation. Both levels of security are made of an anchored steel stabilization structure. The system consists of a spatial supporting steel structure. The front is a steel frame made of HEA100 elements with a protective net, the dimensions of the front are 2.50x2.00 m (40 pcs in total). In the body of the backfill, there is a hidden support tie rod - ground anchor. The stabilizing steel structure is completed in the lower floor at its beginning and end with the help of gravity gabion retaining walls (Fig. 2 right).

Figure 1. From left – outlet of prefabricated drains at the foot of the landslide; realization of horizontal drainage wells; surface rigol and control shaft

Figure 2. Left: View of the retaining wall - two-stage steel anchored structure; Right: The lower basket of the gabion retaining wall

Conclusion

Remedial works were carried out as part of immediately implemented emergency measures. The stabilization of the landslide area was solved comprehensively, starting with additional research works, which refined the engineering geological, hydrogeological, and geotechnical conditions of the area, through the design of remediation to their implementation. On the landslide, geotechnical monitoring consisting of inclinometric measurements, regime observations, geodetic measurements, and measurements of the yield of drainage wells was designed and is ongoing.

Acknowledgments:

This research was partly funded by the Agency of the Ministry of Education, Science, Research and Sport of the Slovak Republic, VEGA, grant project No. 1/0182/23 "Quantification of landslide risk in urbanized areas of Slovakia threatened by the devastating effects of slope movements" and VEGA 1/0180/24 „Application and evaluation of the results of multifunctional analysis of surface seismic waves (MASW) in geological engineering and geotechnical tasks".

STABILITY ASSESSMENT OF HIGH CLIFF SLOPES IN CARBONATE ROCKS - A CASE STUDY, KINGDOM OF SAUDI ARABIA

MOHAMMED MUSTHAFA KHALEEL[1], MOHAMMED JALALUDDIN AHMED[2], KURIAN JACOB[3]

[1] *Arab Centre for Engineering Studies Dubai, United Arab Emirates, k.musthafa@aces-int.com*

[2] *Arab Centre for Engineering Studies Dubai, United Arab Emirates, m.ahmed@aces-int.com*

[2] *Arab Centre for Engineering Studies Dubai, United Arab Emirates, k.jacob@aces-int.com*

Introduction

The proposed Project, spread over an area of 7km2, located in the Kingdom of Saudi Arabia, is bound by a 20 -25 m high, over 5 km long cliff section to the west of the high land. The stability of the cliff slopes have a bearing on the short-term safety and performance of the structures close to the cliff line. The study performed to ascertain the stability of the 'cliff/ escarpment' is considered in the design of the Emergency Vehicular Access (EVA) route and the utility corridor serving the open areas bounded by the Historical Walls along the top of the escarpment.

Methodology

The methodology included acquisition of field data, including geological mapping aided with the satellite imageries to decipher the presence of geological features like faults, shear zones, discontinuities with their orientation with respect to the escarpment. Mapping of cliff face and the area in a width of 100 m along the cliff line was carried out deploying suitable equipment's/ techniques like GPS with rover, terrestrial photography etc. The azimuthal data of the discontinuities/ joints were collected; besides, the joint parameters/ features and laboratory testing like direct shear tests along the identified potential discontinuities. The data was synthesized using the rocscience software's to check the kinematic admissibility, identify the failure modes and the potential blocks. Analytical checks for the for the potential blocks were carried out and global stability checks using slope/W programme, targeting a Safety Factor of 1.5 and 1.2 for static and dynamic conditions.

Geology

The veering cliff line and the high land areas exposes the Jurassic formations (ref 3) which includes the Jubaila Limestone (Ji)- a cream coloured compact limestone with interbeds of calcarenite and thin dolomitic units of Kimmeridgiam age near the top. The Hanifa Formation (Jh)- cream and tan soft limestone with minor interbedded marl and tan clay shale; several brown calcarenite beds, partly Oolitic in middle and upper parts are also noticed. The distinctive geo-structural features noticed are mostly the bandings/ beddings with continuity or discontinuity.

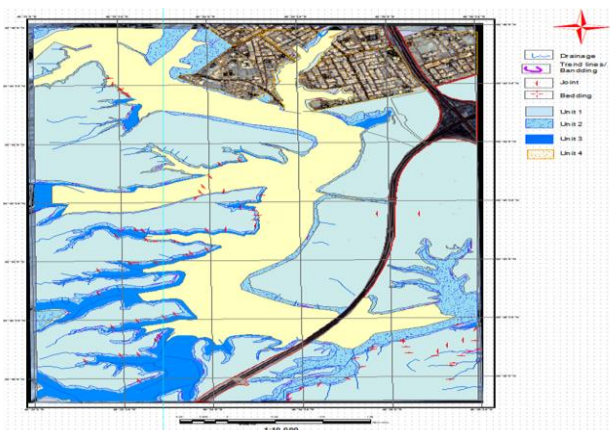

Figure 1. Satellite imagery based geological map of the area

Figure 2. Aerial view of the project location

The valley/ wadi area to the west of the high land, could be a strong erosional feature along mega structural elements, but due to extensive anthropological interventions the elements are camouflaged. The structural elements delineated are Joints/ discontinuities and form lines of beddings. The Cliff line is broadly controlled by the differential erosion activity along the major joints/ fracture system in the area i.e. the N-S to NNE - SSW and E-W fracture systems at large. No such major fault lines / shear zones are discernible in the study area of the project. A 2 – 5 m wide highly destressed zone along the cliff line is manifested by dilated vertical joints with infillings of silt and sand, block movements/ rotations etc.

Rock mass characterisation

The rock mass on the surface in general are unweatherd to slightly weathered (Class-I/II). The effects of weathering are seen along the joints / discontinuities with coatings and in-fillings of clayey to silty material. The rock mass beyond a depth of 1 – 1.5 m are fresh (class I). The thin inter bedded siltstone in general is moderately to highly weathered (Class III/ IV) up to a depth of 5 m from surface (as noticed on the cliff face). Over 36 locations were identified (geopoints G1, G2, G3...etc.) along the cliff edge and the toe line for data collection. From each of these locations 20 – 70 Joint data with the specified parameters were collected. Based on the bore hole logs and the results of geological mapping/ study of the cliff sections, the rock mass was classified in to two categories as Rm1 and Rm2

Keeping in view the commonality of the joint sets, their surface characteristics and the potentiality/ vulnerability of the cliff edge, the locations were clubbed to form Seven structural zones (ZI, ZII...ZVII) for further assessments and analysis (table 1). Each zone covers the 25 m high cliff face and a width of 120 m from cliff edge, respectively.

Slope Stability Analysis: The data was synthesized using the Rocscience software's to the carry out the Kinematic admissibility check and identify the failure modes (ref 2).

Table 1. Kinematic admissibility checks

Structural Zone (Z)	Joint Set combination	Wedge No	Azimuth of joint sets (°)	Azimuth of slope (°)	Input parameters	Analysis remarks
	J1, J3	ZI/W1	031/72,007/84	075/80	γ=2.5 t/m3	
	J1, J4	ZI/W2	031/72,187/88	(E-W cliff)	ϕ° Average=24	
Z-I	J5, JR1	ZI/W3	292/88,310/70		ucs= 40 MPa	
	J6, JR1	ZI/W4	096/87,310/70		E=35	
	JR1	P1	060/81		g=0.17	
Z-II	No Failure Mode				Water pressure =50% in	
Z-III	J1, J3	ZIII/W1	306/17,185/80	300/40	tension cracks	
	J1	ZIII/P1	306/17	(N-S Cliff)		
Z-IV	Not considered for slope stability analysis					
Z-V	No wedge/planar failure found					
Z-VI	Not considered for slope stability analysis					
	J1, J2	ZVII/W1	312/22,176/86	310/40		
Z-VII	J1, J3	ZVII/W2	312/22,359/85	(N-S Cliff)		
	J1, J4	ZVII/W3	312/22,290/81			
	J1	ZVII/P1	312/22			

Table 2. Output of Analitical checks

Zone	Block No.	FoS (1)	Slope Protection/ Treatment Measures				FoS (2)	FoS (3)	Wedge weight. (t)	Wedge volume. (m3)	Remarks
			Rockbolt								
			Length (m)	Ancr length (m)	Capacity (t)	Shotcrete (mm)					
Z -I	ZI-W1	1.48	-	-	-		1.48	1.44	2.62	1.04	Safe
	ZI-W2	2.12	-	-	-	-	2.12	2.08	2.07	0.87	Safe
	Z1-W3	2.39	-	-	-	-	2.39	2.05	23.80	9.55	Safe
	Z1-W4	1.45	-	-	-	100	22.0	21.17	16.34	6.53	Safe

Z-III	ZIII-W1	-	-	-	-	-					WnF(4)
	ZIII -P1	2.65	-	-	-	-	2.65	1.71	348	139	Safe
Z-VII	ZVII-W1, W2, W3 & W4	-	-	-	-	-	-	-	-	-	WnF(4)
	ZVII / P1	1.82	-	-	-	-	1.82	1.20	17	41	Safe

FoS (1) Static (without support or seismic effects), indicating the likely risk of instability under own wt, water pressure, and external loading without introducing support (Anchor).
FoS (2) Static with support, as necessary to achieve the target safety factor.
FoS (3) Dynamic EQ effects (with 0.17 g). T was adjusted, if required such that minimum target safety factor is satisfied
WnF (4) Wedge block not Formed

Analytical checks for the potential blocks and global stability checks using *Rocscience* and *slope/W* programmes were carried out respectively targeting a Factor of Safety of 1.5 and 1.2 (ref 1) for the respective static and dynamic conditions. The profiles (S1 - S8) were checked for global stability using a FEM model study by circular failure analysis- Morgenstern method using *slope/W* programme, with a surcharge load of 35 tons at the cliff top. A typical analysis of section Z-II/ S1 –17.5m slope height is given below.

Typical stability analysis for slope S1 – Z-II of 17.5m height

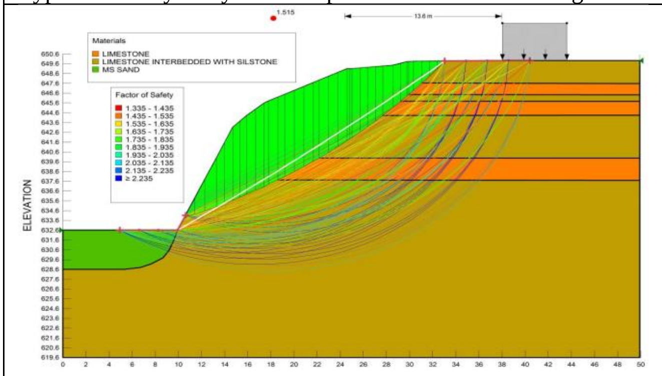

Summary of output from Global stability check

Section ID	***Factor of Safety***	
	Static	***Dynamic / Earthquake***
SECTION 1	*1.515*	*1.197*
SECTION 2	*1.516*	*1.210*
SECTION 3	*1.512*	*1.189*
SECTION 4	*1.491*	*1.223*
SECTION 5	*1.495*	*1.289*
SECTION 6	-	
SECTION 7	*1.491*	*1.198*
SECTION 8	*1.809*	*1.387*

Figure 3. Outputs of Global Analysis

Conclusion and Recommendations:

The above analytical check reveals that in general the wedges formed show high FoS (+2) and are expected to be stable due to their high shear strength characteristics and relatively low/ sub-horizontal beds. No such support system was required for the stabilization of the cliff slopes with foundation/ structural loadings of 35t. The cliff slopes have potential/ unstable wedges in the 2 – 3 m wide de-stressed zone along the cliff edge and locally on the slope face. These wedge blocks are likely to get dislodged/ slide down with time, due to the in fillings in the dilated joints and eventual charging with rain water. The natural slopes by virtue of it's gentle to moderate slope angles of 45 – 50^{o} with the sub-horizontal/ gently dipping (2 – 5^{o}) bedding planes (J2) provide relatively stable conditions for the cliff.

Keeping in view the compulsions of the heritage site, specific recommendations on slope stabilization (without shotcrete, guniting, mesh, anchors) like use of synthetic grouts or pinning the loose blocks locally with rock bolt were advised. Based on the evaluations and the manifestations of a 2 – 5 m wide distressed zone along the cliff line a safe set back distance of 5 - 8m from the escarpment edge has been recommended.

References

1. Duncan C. Wyllie**,** *Foundations on Rock (2nd Edition),* E&FN Spon. 1999
2. Hoek. E and Bray.J.W, *Rock Slope Engineering (Revised third edition)***,** Institution of Mining and Metallurgy, U.K, 1999.
3. Richard A. Bramkamp, Leon F. Ramirez, Geology of the Northern Tuwayq Quadrangle, KSA, USGS Publications Warehouse, 1958.

A GEOTECHNICAL APPROACH FOR ENHANCING THE COASTAL VULNERABILITY INDEX (CVI) METHODOLOGY: APPLICATION IN THE GULF OF PATRAS, GREECE

VASILEIOS BOUMPOULIS[1], NIKOLAOS DEPOUNTIS[1], GEORGE PAPATHEODOROU[1]

[1]Department of Geology, University of Patras, Greece, vasileios_boumpoulis@ac.upatras.gr

Introduction

Coastal zones are one of the most complex and dynamic systems since their landform changes rapidly due to the combined action of tidal flows, currents and waves on coastal sediments (Raper et al. 2005; Boumpoulis et al. 2023). One of the most common and diachronic problems in coastal zones is the coastal erosion. In Greece, more than 20% of its total shoreline (EC 2004; Boumboulis et al. 2021) is threatened by coastal erosion and rising sea levels. Coastal Vulnerability Index (CVI) is one of the most used methods to assess coastal vulnerability to sea-level rise (SLR) driven erosion. However, numerous methodological gaps in the CVI approach can be found in the literature, especially in local scale areas. For this reason, this study aims to construct a coastal vulnerability assessment conceptual framework to improve the outcomes of CVI in local scale areas. To achieve this, an index model named as Geotechnical Coastal Vulnerability Index (GCVI) is used, which incorporates two geotechnical variables in the calculations, the geotechnical identification and the median grain size distribution (D50), as well as the presence of P. Oceanica. The use of those parameters seems to improve the quantification of coastal resistance to erosion and seems to be more accurate in the calculations of CVI in local scale areas. As a local scale (pilot) area to apply this approach it was used the Gulf of Patras in Western Greece, which is suffering erosion problems due to climate change and human intervention.

Methods

The selected key variables of GCVI used in this study are: i) the geotechnical identification, ii) the median grain size distribution (D50) of coastal sediments, iii) the significant mean wave height, iv) the coastal slope, v) the presence of P. Oceanica and vi) the average tidal range.

To calculate the geotechnical variables, a thorough geotechnical investigation was carried out in the research area, including drilling of boreholes, laboratory and in-situ geotechnical tests (Standard Penetration Test-SPT), numerous coastal sediment sampling and field engineering–geological mapping. The synthesis of those collected data led to the creation of a local scale geotechnical map of the pilot area. This map classifies the geological formations of the coastal zone according to their geotechnical characteristics and their erosion resistance that is used in the GCVI model.

The final integration of geotechnical variables into the numerical calculation of the index for classifying the shoreline into different vulnerability classes, performed via the total number of blows SPT for the variable of geotechnical identification. While for the median grain size distribution (D50) variable, the spatial distribution of the D50 value estimated using the optimal spatial interpolator method, as it is described in Boumpoulis et al. (2023). For the weighting of each one of the six variables used in the GCVI model, the Principal Component Analysis (PCA) method was implemented. For the validation of the results, the rate of the historical shoreline movement (m/y) was used, by constructing the receiver operating characteristic (ROC) curve and computing its area under the curve (AUC) value.

Results

The spatial distribution of the GCVI along the shoreline of the pilot area (Figure 1) shows that the coastal Zone 1, the greater part of Zone 4 and half of Zone 8 have a very high vulnerability level. Moreover, the coastal Zone 5, the western part of Zone 4, small parts of Zone 7 and the central part of Zone 8 have a high vulnerability level. In addition, the coastal Zone 1, the western and eastern part of Zone 3, Zone 6 and a small part of Zone 7 have a moderate vulnerability status. Finally, the central part of Zone 3, Zone 5 and the western part of Zone 2 are characterized by very low and low vulnerability regime. The validation results, represented by ROC curves and AUC values, indicated that the parameter for the rate of historical shoreline movement and the PCA method achieved a 67.57% accuracy. This is considered as satisfactory percentage compared to similar coastal vulnerability models, which achieve around 68.9% (Fu et al. 2022).

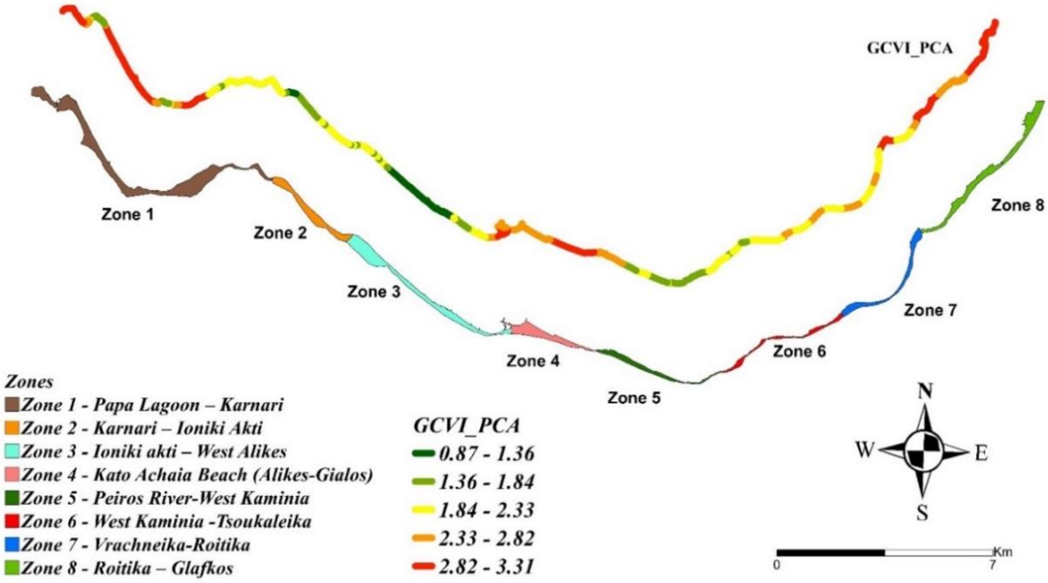

Figure 1. Spatial distribution of GCVI along the shoreline of the Gulf of Patras.

Conclusion

In the literature, several efforts have been made to improve coastal vulnerability models, especially the CVI, which is the best-known model to calculate vulnerability. A first attempt towards the improvement of those uncertainties, is the quantification of resistance to erosion variable with the use of geotechnical data instead of geological data in the CVI calculations for the research area (Boumboulis et al. 2021). Moreover, the classical formulation of CVI with the use of i) geological, ii) historical shoreline movement, iii) the significant mean wave height, iv) the coastal slope, v) sea level rise and vi) the average tidal range and the absence of weigh factors in the relvant calculations may underestimate the vulnerability and this fact is mentioned also in other papers (De Serio et al. 2018). In this study the use of six variables, with an emphasis given in the geotechnical variables and the presence of P. Oceanica, along with the introduction of weight factors using PCA, seems to increase the reliability and accuracy of the vulnerability model, as each variable has a different contribution to vulnerability assessment. Futhermore, a validation model was developed using the rate of the historical shoreline movement to assess how accurately the model values reflect to reality, since in most of the relevant research studies there is not proposed a standard procedure for verifying the predictions in CVI models.

References

Boumboulis V, Apostolopoulos D, Depountis N, Nikolakopoulos K (2021) The Importance of Geotechnical Evaluation and Shoreline Evolution in Coastal Vulnerability Index Calculations. J Mar Sci Eng 9:423. https://doi.org/10.3390/jmse9040423

Boumpoulis V, Michalopoulou M, Depountis N (2023) Comparison between different spatial interpolation methods for the development of sediment distribution maps in coastal areas. Earth Sci Informatics 16:2069–2087. https://doi.org/10.1007/s12145-023-01017-4

De Serio F, Armenio E, Mossa M, Petrillo AF (2018) How to define priorities in coastal vulnerability assessment. Geosci 8:1–20. https://doi.org/10.3390/geosciences8110415

EC [European Commission] (2004) Living with Coastal Erosion in Europe – Sediment and Space for Sustainability. OPOCE, Luxembourg. http://www.eurosion.org/project/eurosion_en.pdf (accessed July 2016).

Fu GW, Cao C, Fu KZ, et al (2022) Characteristics and evaluation of coastal erosion vulnerability of typical coast on Hainan Island. Front Mar Sci 9:1–19. https://doi.org/10.3389/fmars.2022.1061769

Raper J, Livingstone D, Bristow C, McCarthy T (2005) Constructing a Geomorphological Database of Coastal Change Using GIS. Coast Mar Geo-Information Syst 399–413. https://doi.org/10.1007/0-306-48002-6_28

BACK ANALYSIS OF CUT SLOPES ALONG THE FAST TRACK ROAD OF NEPAL

UJJWAL KRISHNA RAGHUBANSHA [1], RANJAN KUMAR DAHAL [2]

[1] *Central Department of Geology,Tribhuwan University, raghubanshiujjwal@gmail.com*

[2] *Central Department of Geology,Tribhuwan University, rkdahal@gmail.com*

Introduction

Slope stability is the major problem in mountainous country either natural or engineered slopes. The detailed study of topography, geology, shear strength, groundwater conditions, external loading and plan curvature of the slope are an important parameter for slope stability analysis. There are various challenges in making the Cut Slopes on landslide made landscape.

This study is mainly focused on the back analysis of cut slope failure, stability analysis and inventory mapping of cut slope/cut slope failures. Traditional slope stability analysis involves predicting the location of the critical slip surface of the slope and calculation of FOS at that location. Back analysis technique can be used in a deterministic and probabilistic analysis to find all possible failure mechanisms, FOS and reliability indices. Slope seepage analysis is modeled as the finite element through transient seep/w using different parameters such as hydraulic conductivity of soil and rock, grain size analysis, liquid limit, volumetric water content, and extreme monsoon rainfall. Similarly, soil slope stability is analyzed using slope/w limit equilibrium method using strength parameters, such as friction angle, cohesion and pore-water pressure from seep/w. kinematic analysis is carried out in discontinuous rock mass. Back analysis is carried out in cut slope failure assuming Factor of Safety (FOS) as 1 under consideration of trial values of strength parameters through probabilistic and sensitivity method.

Methods

The limit equilibrium analysis is a conventional method used for analyzing slopes assessing the balance between external forces acting on the slope and the internal forces resisting failure along the potential failure surface. This methodology yields findings that are reasonably accurate and dependable for simple material strength behavior with the calculation of a safety factor, which is important for assessing the sensitivity of potential future conditions of slope. However, a different method for studying slope stability known as finite element analysis preserves global equilibrium up until the slope fails while making fewer assumptions about the failure cause. This approach is helpful for providing precise and flexible information regarding deformation at operating stress levels and failure.

Geological sections are made based on drillings and various geophysical investigations and lab works for the back analysis of cut slope failure. Slide 2D software was used. The deterministic analysis was carried out using the mean of all the input parameters to find one critical failure surface. Among the available LE methods, Bishop Simplified Method (BSM) was used as it is the most suitable for a circular failure.

Results

The back analysis of geological parameters at failure portion considering the factor of safety 1.5 for dry condition. The reduced geological parameter at failure locations is taken based on the sensitivity analysis. In the sensitivity analysis among cohesion and friction angle, friction angle is more sensitive, it indicates that small changes in the value of friction angle can have a larger impact on the overall stability of the slope compared to small changes in the value of cohesion. This is because the shear strength of the slope is more influenced by friction angle than cohesion.

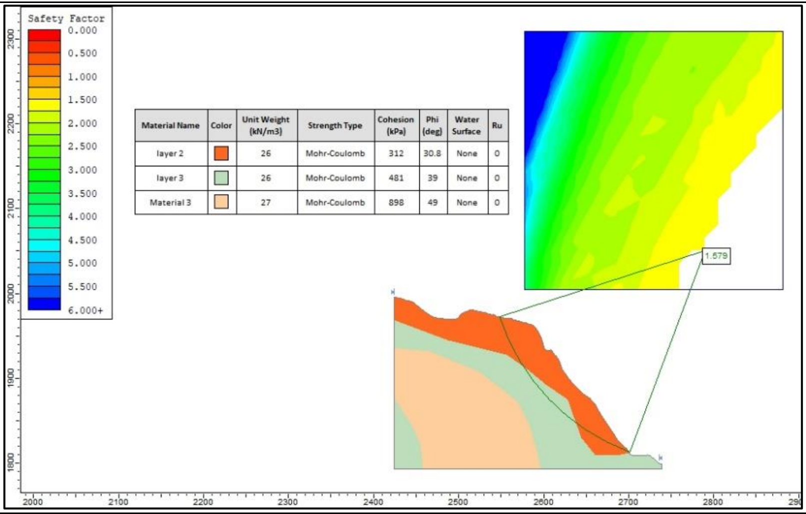

Figure 1: Back Analysis of profile

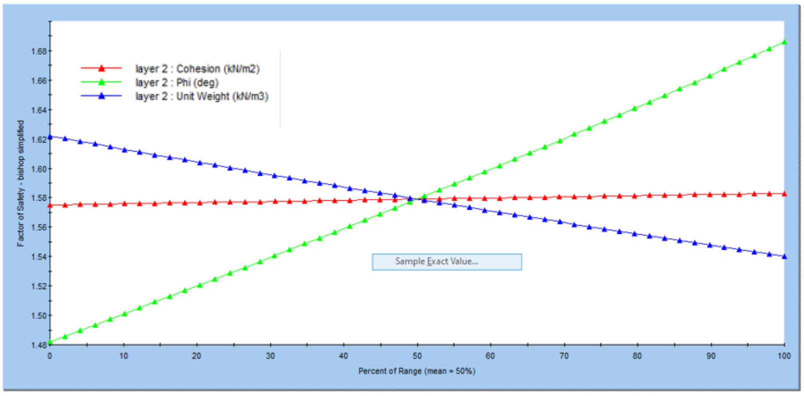

Figure2: Combined sensitivity plot of FOS vs friction angle cohesion and Unit weight

Conclusion

A comprehensive back analysis and stability assessment of the cut slopes were done for slope stability. Sensitivity analysis and probabilistic approach of stability analysis was used to analyze the slope failure. Limit Equilibrium method was used for stability analysis. Bishop Simplified Method (BSM) analysis was carried out to determine the factor of safety.

References

Abramson, L. W., Lee, T. S., Sharma, S., & Boyce, G. M. (2002). Slope stability and stabilization methods. John Wiley & Sons.

Barton, N. (1976). The Shear Strength of Rock and Rock Joints. In Int. J. Rock Mech. Min. $ci. & Geomech. Abstr (Vol. 13). Pergamon Press.

Bishop,A.W. (1955). The use of slip circles in the stability analysis of slopes. Géotechnique, 7-17.

Cheng, Y.-M., Wei, W.-B., & Wang, X.-M. (2007). Dynamic response of a high rockfill dam in an earthquake. Soil Dynamics and Earthquake Engineering, 27(8), 749-763

Duncan, J. M., Wright, S. G., & Brandon, T. L. (2008). Limit equilibrium and finite- element analysis of slopes. Geotechnique, 58(7), 537-546.

Edgers, L., & Nadim, F. (2004). Rainfall-induced slides of unsaturated slopes. InLandslides: evaluation and stabilization (pp. 1091-1096).

Fellunius, W. (1936). Calculations of the Stability of Earth Dams. Proceedings of the second Congress of Large Dams. Vol. 4, pp. 445-63, Washington D. C.

Hatheway, A. W. (1996). Slope Stability and Stabilization Methods. In Environmental & Engineering Geoscience: Vol. II (Issue 3, pp. 447–449).

Michalowski, R. L. (1995). Limit equilibrium method of stability analysis. In B. R. Singh (Ed.), Principles of geotechnical engineering (pp. 214-270). CRC Press.

IMPACT OF DEEP-SEATED ROCK SLIDES ON INFRASTRUCTURE

CHRISTIAN ZANGERL [1]

[1] *BOKU University, Department of Civil Engineering and Natural Hazards, Institute of Applied Geology, Peter Jordan-Strasse 82. 1190 Vienna, Austria, christian.j.zangerl@boku.ac.at*

Introduction

Deep-seated rock slides affecting entire valley slopes and reaching volumes of millions of m^3 are frequently observed in mountainous regions. This type of landslide displaces at velocities in the range from extremely slow to extremely rapid (Zangerl & Strauhal 2020) and the deformation is localised along one or several shear zones where most of the measured total slope displacement accumulates. These shear zones reach thicknesses in the range of a few decimetres to tens of meters and are composed of uncemented fault breccias and gouges, with a spatially heterogeneous arrangement (Strauhal et al. 2017). Concerning slow moving rock slides, if active or reactivated over longer periods of time, they can adversely affect settlements and infrastructure due to differential and localised displacements of the ground surface and subsurface. Even for very slow movements the damage can be considerable and the life-cycle of man-made structures can be reduced, accompanied with a great economic loss. In some rare cases there is also the danger of a sudden slope failure with acceleration to high velocities and the transition to long runout flow-type rock avalanches, in the worst case leading to a catastrophic event.

This study presents an overview and summary of mechanisms how slowly moving deep-seated rock slides can interact with infrastructure, such as dam reservoirs, high- and railway foundations and bridges, penstocks, headrace tunnels, water supply and transportation tunnels. Using selected, well-studied case studies from the Alps, the underlying interaction processes between infrastructure and deep-seated rock slides are shown in detail, emphasizing the role of cascading and interconnected processes (Mani et al. 2023), as well as the increasing relevance of climate change factors.

Methods

The case studies presented herein include comprehensive analyses of the failure and deformation processes in relationship to the infrastructure based on a broad spectrum of applied methods, comprising geological-geomorphological field surveys, GIS-based terrain analyses, in-situ investigation by core drilling, drift construction and geophysical exploration, surface and subsurface deformation and hydrogeological monitoring, and numerical modelling techniques. Results from these investigations and measurements are presented in the context, how the geological-hydrogeological situation, the geometry and kinematics, as well as the different influencing factors can affect the stability and the temporally variable deformation behaviour of a rock slide.

Results

Reactivation and/or acceleration of existing rock slides or slabs thereof are often observed in connection with the construction of infrastructure, leading to differential and localized displacements of the ground. The triggers for this can be based on natural or construction related factors, or a combination of both, including extreme rainfall and snow melt events, erosion at the foot by flooding, the initial infilling of a reservoir or the rapid drawdown, construction of a cut slope, loading of the slope by the infrastructure building itself, and others. In addition, frequently observed ongoing slope movements, even with an extreme low level of activity, can have an adverse impact on the structure over long periods of time and require early recognition, comprehensive planning, and if necessary, action.

Deep-seated rock slides can adversely affect dam reservoirs in various ways. One possibility is that an abutment of the dam is located in a rock slide mass which is moving (Schuster 2006). This results in a narrowing of the valley leading to a progressive deformation of the structure, often accompanied by the formation of cracks (Barla 2018). In this context, the movement of the rock slide can be triggered or accelerated by the initial impounding of the reservoir or its drawdown. Moreover, the progressive

deformation of the abutments can lead to unfavourable seepage behaviour below the dam structure. The instability of abutments and foundations, especially during the construction phase of a dam, is a further interaction mechanism that needs foresighted planning and mitigation measures (Dini et al. 2020). Impact also may occur when rock slides gradually reduce the storage space of the reservoir or threaten the infrastructure and its surroundings through sudden high-velocity rock slide events. In particular, the initial impoundment can lead to reactivation and/or acceleration of pre-existing rock slides, which requires measures such as continuous monitoring or even the construction of slope drainage drifts to maintain operational safety (Zangerl et al. 2024).
Deep-seated rock slides can affect penstocks, headrace and water supply tunnels, as well as highway and railway tunnels. Penstocks and headrace tunnels as essential components of hydropower plants or drinking water supplies can be impacted in their service life by very slow-moving rock slides due to localised shear deformation (Barla 2018, Leblhuber & Bonapace 2013, Poisel et al. 2015). On the one hand, very low movement rates of a few mm/year can accumulate over a long period of time and exceed the structural limits with regard to deformation, and on the other hand extreme meteorological and/or hydrological events can trigger reactivations or accelerations.
The impact of deep-seated rock slides on road/highway and bridge foundations mainly involve localized deformations of the slope flanks, leading to sliding and toppling mechanism of the structure. Inactive rock slides that are reactivated by extreme meteorological events or slope foot erosion due to flooding are particularly critical. In this context, a case study from Austria, where a flood event from 2005 triggered and reactivated pre-existing rock slides or slabs, causing damage of main roads and bridges as well as headrace drifts and penstock of a hydropower plant, will be presented.

Conclusion
The implications of this study are manifold and emphasize the high relevance of reliable feasibility studies and the consideration of overlapping cause and triggering factors, as well as cascading and compound effects in order to avoid subsequent problems during the construction and operation phase, and to achieve the planned service life and infrastructure safety.

References
Barla, G. Numerical modeling of deep-seated landslides interacting with man-made structures. Journal of Rock Mechanics and Geotechnical Engineering, 2018, 10(6), 1020-1036.

Dini, B.; Manconi, A.; Loew, S.; Chophel, J. The Punatsangchhu-I dam landslide illuminated by InSAR multitemporal analyses. Scientific reports, 2020, 10(1), 8304.

Leblhuber, P.; Bonapace, P. New penstock at the Kaunertal hydropower station–site investigation and grouting concept. Geomechanics and Tunnelling, 2013, 6(5), 446-455.

Mani, P.; Allen, S.; Evans, S.G.; Kargel, J.S.; Mergili, M.; Petrakov, D.; Stoffel, M. Geomorphic Process Chains in High-Mountain Regions—A Review and Classification Approach for Natural Hazards Assessment. Reviews of Geophysics, 2023, 61(4), e2022RG000791.

Poisel, R.; am Tinkhof, K.M.; Preh, A. Die Interaktion Großhangbewegungen–Tunnel am Beispiel eines Lehnenstollens in 370 m Seehöhe. Österreichische Ingenieur- und Architekten-Zeitschrift, 2015, 160, 221-230.

Schuster, R.L. Interaction of dams and landslides: case studies and mitigation. Reston, Virginia: US Geological Survey, Professional Paper, 2006, 1723, 107p.

Strauhal, T.; Zangerl, C.; Fellin, W.; Holzmann, M.; Engl, D. A.; Brandner, R.; Tropper, P.; Tessadri, R. Structure, mineralogy and geomechanical properties of shear zones of deep-seated rockslides in metamorphic rocks (Tyrol, Austria). Rock Mechanics and Rock Engineering, 2017, 50, 419-438.

Zangerl, C.; Strauhal, T. Investigations and monitoring of deep-seated rock slides in feasibility studies for dam reservoirs. AUC GEOGRAPHICA, 2020, 55(2), 210-217.

Zangerl, C.; Lechner, H.; Strauss, A. Influence of Rock Slide Geometry on Stability Behavior during Reservoir Impounding. Applied Sciences, 2024, 14(11), 4631.

SFM PHOTOGRAMMETRY FOR ROCKFALL MONITORING AND HAZARD ASSESSMENT ALONG ROAD NETWORKS. THE CASE IN AGRAFA REGION, CENTRAL GREECE

THEMISTOKLIS CHATZITHEODOSIOU [1], IOANNIS FARMAKIS [2], DIMITRA PAPOULI [1], GEORGE STOUMPOS [1], GEORGE PROUNTZOPOULOS[3], VASSILIS MARINOS [1]

[1] *National Technical University of Athens, Greece, chatzitheodosiou@mail.ntua.gr*

[2] *University of Newcastle, Australia, i.farmakis@icloud.com*

[3] *Independent Geotechnical Engineering Consultant, Greece, gproun@gmail.com*

Introduction

Rockfalls pose a major threat to transportation in mountainous regions, particularly in tectonically disturbed limestone areas like central Greece (Marinos, 2010). Remote sensing technologies, such as Structure-from-Motion (SfM) photogrammetry (Westoby et al., 2012) and Terrestrial Laser Scanning (TLS) LiDAR, have improved hazard assessment by providing high-resolution data for terrain and rockfall analysis (Kromer et al., 2019; Chatzitheodosiou et al., 2024). This study examines the Agia Varvara-Agrafa region in Evritania, Greece, where complex geology consisted of heterogenous and tectonised rock masses create conditions for frequent rockfalls along a critical mountain road. A large wedge-shaped rockslide in this area has exposed disturbed rock masses, resulting in continuous smaller rockfalls and new slides that pose significant risks to road safety.

Methods

Over a two-year period, with monitoring intervals of four months, SfM photogrammetry was utilized to capture the evolution of susceptible slopes through high-resolution UAV imagery. This method generated precise point clouds, enabling detailed analysis of geomorphological changes and creating a time series of terrain evolution. The M3C2 algorithm (Lague et al., 2013) was applied for accurate quantification of rockfalls and slope deformations. Additionally, spatial clustering through the DBSCAN algorithm (Ester et al., 1996) and volumetric measurements via the Iterative Alpha Shape algorithm (DiFrancesco et al., 2021) contributed to the development of a comprehensive digital rockfall database. This database enhanced the understanding of landslide dynamics in the region.

Results

The methodology identified potential rockfall sources, tracked failure kinematics, and estimated potential failure volumes. It provided essential data for designing effective rockfall mitigation strategies, improving safety on the Agia Varvara-Agrafa road. Potential failures ranged from 5 to 30 m^3 for occasional detachments from upper slopes, and 1 to 2 m^3 for more frequent smaller rockfalls. The accurate projection of failure locations and consistent post-failure assessments confirmed the effectiveness of this approach in managing rockfall hazards.

Conclusion

This study demonstrates that SfM photogrammetry and associated methods can significantly enhance the risk management of transportation corridors in geologically complex terrains by informing targeted mitigation strategies. The approach is broadly applicable to similar geological settings, contributing to improved infrastructure safety.

References

Chatzitheodosiou, T. "One rock at a time" 3D Geology Mini-Series. *Available online:* https://sketchfab.com/themisto123 *(accessed on February 2024).*

Chatzitheodosiou, T.; Farmakis, I.; Prountzopoulos, G.; Papouli, D.; Stoumpos, G.; Marinos, V. Addressing rockfall challenges in flysch environment - A case study from Greece. In *Proceedings of the 6th Regional Symposium on Landslides in the Adriatic-Balkan Region, ReSyLAB2024, Belgrade,* Serbia,

15–18 May 2024; pp. 283-289.
DiFrancesco, P.M.; Bonneau, D.A.; Hutchinson, D.J. Computational geometry-based surface reconstruction for volume estimation: a case study on magnitude-frequency relations for a LiDAR-derived rockfall inventory. *ISPRS International Journal of Geo-Information.* 2021, 10.
Ester, M.; Kriegel, H.P.; Sander, J.; Xu, X. A density-based algorithm for discovering clusters in large spatial databases with noise. In *Proceedings of the KDD-96 Conference*, Portland, Oregon, 2–4 August 1996.
Kromer, R.; Walton, G.; Gray, B.; Lato, M.; Group, R. Development and optimization of an automated fixed-location time lapse photogrammetric rock slope monitoring system. *Remote Sensing.* 2019, 11.
Lague, D.; Brodu, N.; Leroux, J. Accurate 3D comparison of complex topography with terrestrial laser scanner: application to the Rangitikei Canyon (New Zealand). *ISPRS Journal of Photogrammetry and Remote Sensing*. 2013, 82, 10–26.
Marinos, V. New proposed GSI classification charts for weak or complex rock masses. *In Proceedings of the 12th International Congress of Geological Society of Greece; Bulletin of Greek Geological Society*: Patra, Greece, 2010; Volume XLIII, pp. 1248–1259.
Westoby, M.J.; Brasington, J.; Glasser, N.F.; Hambrey, M.J.; Reynolds, J.M. Structure-from-Motion photogrammetry: a low-cost, effective tool for geoscience applications. *Geomorphology*. 2012, 179, 300–314.

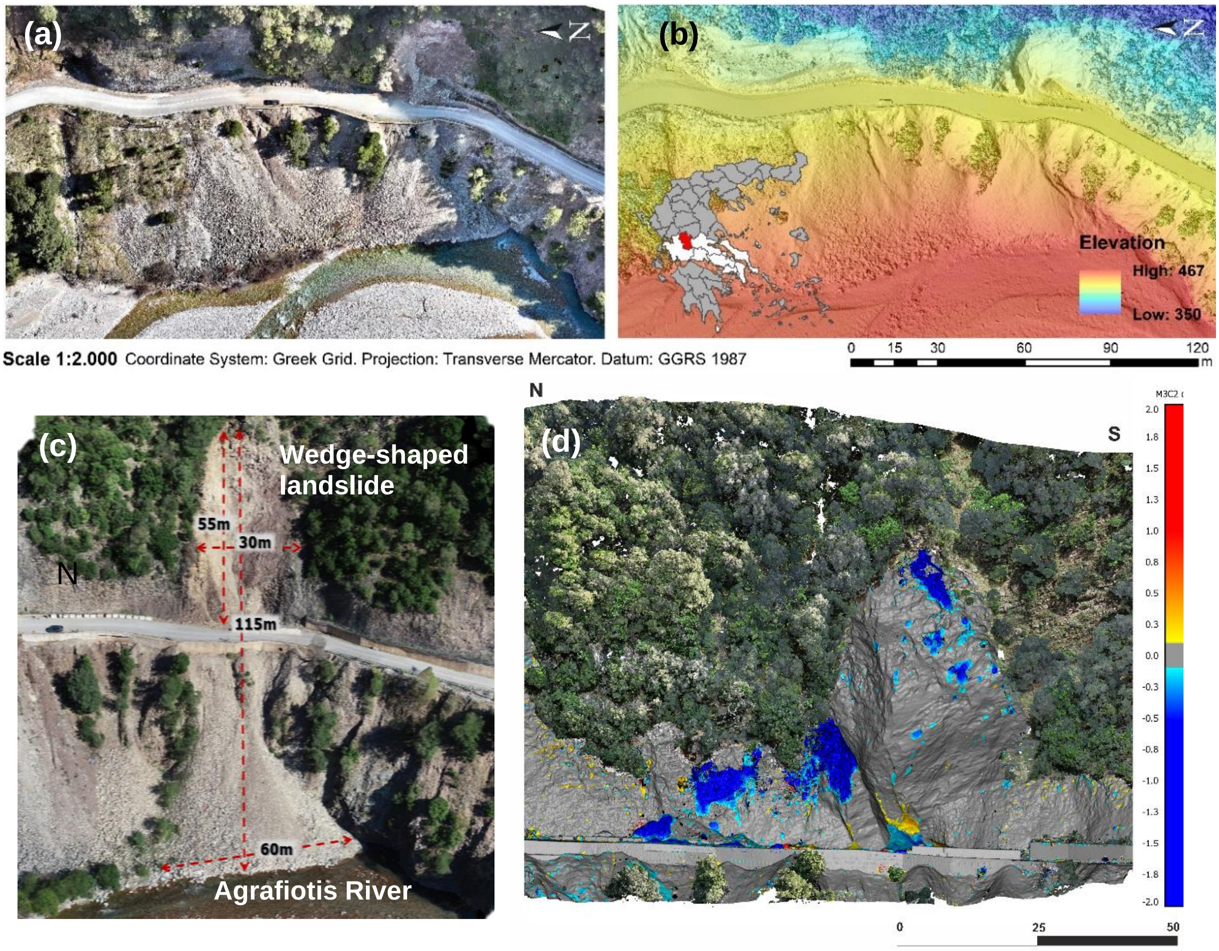

Figure 1. The Agia Varvara - Agrafa study site in Evritania, Central Greece, featuring: (a) an orthomosaic, (b) a Digital Surface Model (DSM) (surveyed on 03 Feb. 2020), (c) an aerial view of the landslide, (d) M3C2 change detection output, depicting negative (loss) and positive (gain) changes presented by cooler and warmer colours, respectively. [For an interactive exploration and detailed visual representation of the Agia Varvara - Agrafa slope, readers are encouraged to visit the latest digital twin online (Chatzitheodosiou, 2023)].

LANDSLIDE SUSCEPTIBILITY TO RAINFALL AT A NATIONAL SCALE IN NEPAL WITH EMPHASIS ON EARLY WARNING

ANANTA MAN SINGH PRADHAN [1], SUCHITA SHRESTHA [2], RENÉ KAHNT[3]

[1] *Ministry of Energy, Water Resources and Irrigation, Government of Nepal, Nepal, anantageo@hotmail.com*

[2] *Department of Mines and Geology, Ministry of Industry, Commerce and Supplies, Government of Nepal, Lainchour, Kathmandu, Nepal, suchitashrestha@gmail.com*

[3] *G.E.O.S Ingenieurgesellschaft mbH, Germany, r.kahnt@geosfreiberg.de*

Introduction

Landslides are becoming increasingly frequent in Nepal due to intensifying precipitation patterns and the expansion of rural road construction. These factors significantly enhance the risk to both lives and livelihoods in the affected areas. To address this pressing issue, this study presents an integrated methodology that combines two advanced modeling techniques aimed at predicting landslide probabilities. The first technique focuses on analyzing historical data and covariates to identify areas prone to landslides. The second technique employs real-time data collection and machine learning algorithms to continuously update and refine the predictions. By merging these two approaches, more accurate and timely forecasts of landslide occurrences can be provided. Additionally, the study proposes the establishment of a near-real-time warning system for landslides. This system is designed to alert communities and authorities about imminent landslide threats, allowing for swift evacuation and disaster response measures. The integration of these modeling techniques and the warning system aims to mitigate the adverse impacts of landslides, enhancing the resilience of communities in Nepal to such natural disasters. Through this comprehensive approach, we hope to safeguard lives and livelihoods against the growing threat of landslides. This research deals with landslide analysis and subsequent development and implementation of local and regional nowcast early warning systems in the Nepal Himalaya.

Methods

In this study, an integrated process based on two different modelling approaches has been applied. First, a probabilistic approach of landslide susceptibility modelling. The initial method employed a probabilistic, explainable artificial intelligence (XAI) strategy, amalgamating Generalized Additive Models with Structured Interactions (GAMI-Net), to forecast the probability of landslide events within geomorphic slope units. These models integrate various causative factors (CFs) and leverage data on geo-environmental factors associated with landslide occurrences. Second, developed a near-real-time landslide warning system coupling the result of landslide susceptibility and decision tree based selection criteria. Terrain analysis-derived independent variables were incorporated to bolster the modeling procedures in this study. Moreover, the adoption of a global Landslide Hazard Assessment model for Situational Awareness (LHASA) (Kirschbaum and Stanley, 2018) aided in pinpointing areas and timeframes with heightened landslide potential within the study region.

The modelling procedures have been supported throughout this research by including independent variables obtained from terrain analysis. All morphometric variables were derived from a detailed Digital Elevation Model (DEM) in 20 × 20 m scale. A LHASA has been used to provide an indication of where and when landslides may be likely around in the study area.

Results

The result of landslide susceptibility map is presented in Figure 1, which includes the spatial distribution of mean probability for landslide susceptibility across slope units based on 5-fold random cross validation process. The landslide susceptibility map was classified using natural break algorithm in GIS platform. A total of 69.72% of the area was categorized as having a very low susceptibility, 16.01% as low susceptible, 6.84% as moderate, 4.07% as high and the remaining 3.36% was considered to have very high susceptibility. About 81.51% of landslide data were located in the very-high-susceptibility class, demonstrating the reliability of the map. This map shows the average likelihood of landslide occurrence for different regions.

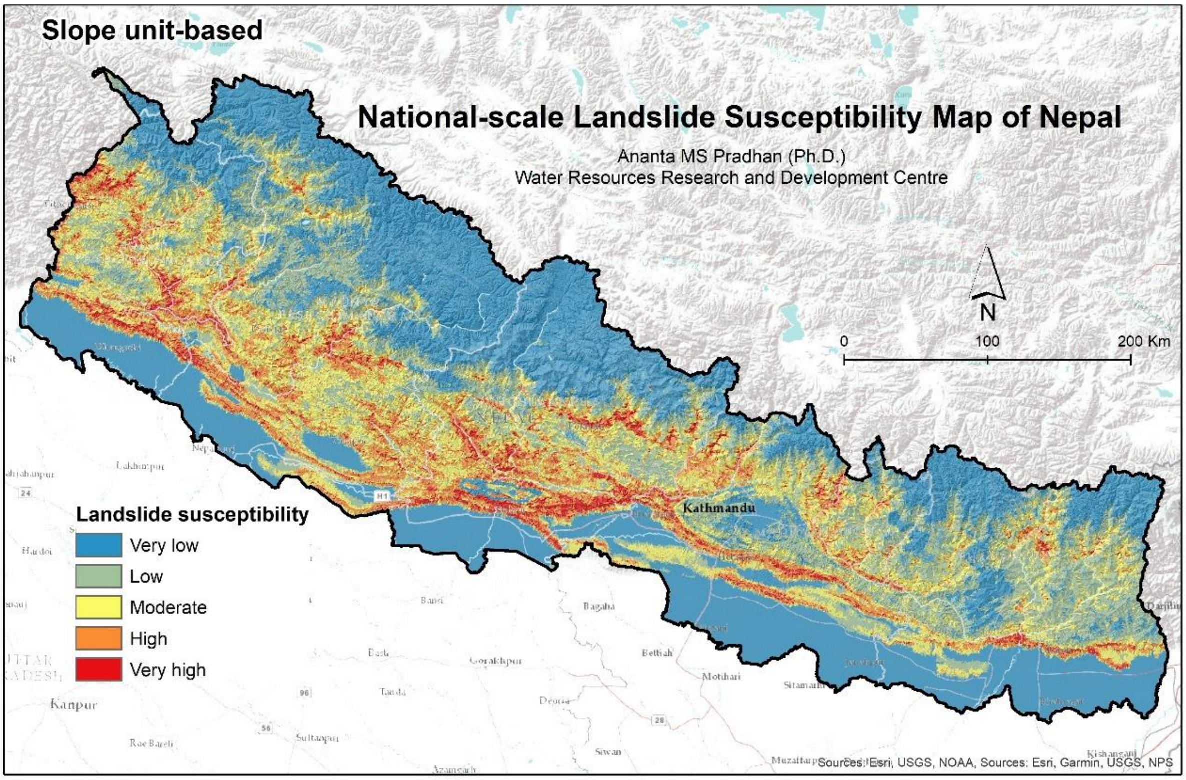

Figure 1. Landslide susceptibilty map of Nepal.

The receiver operating characteristic (ROC) curve was used to evaluate the model and the accuracy of the model was found to be 84%. After preparing the final landslide susceptibility maps, a landslide Nowcast system was developed in Google Earth Engine (GEE) platform and a name "Landslide Hazard Assessment Model LhamNepal) was assign to the developed Application. LhamNepal is an open-access application developed in Google Earth Engine for the rapid characterization of near real time landslide hazard detection to both the scientific and the emergency management communities.

Conclusion

This study significantly advances the field of Landslide Susceptibility Mapping (LSM) by showcasing the potential of advanced machine learning techniques. It underscores the crucial need for precise and interpretable hazard assessments, highlighting their importance in effective disaster management.

References

Kirschbaum, D.,; Thomas, S. Satellite-based assessment of rainfall-triggered landslide hazard for situational awareness. *Earth's Future* 6.3 (2018): 505-523.

LANDSLIDE HAZARD MANAGEMENT IN GREECE: THE NATIONAL LANDSLIDE DATABASE AS A MITIGATION TOOL

NATALIA SPANOU [1], EMMANUEL APOSTOLIDIS [1], KATERINA KAVOURA [1], FOTEINI PANAGIOTIDOU [1], IERONYMAKIS VASILEIOS [1], PANAGIOTA KOKKALI [1], NIKOLAOS NIKOLAOU [1], GARYFALIA KONSTANTOPOULOU [1], PANAGIOTIS PASCHOS [1], ALEXANDROS KEPAS [1]
[1] *Hellenic Survey of Geology and Mineral Exploration, Greece;* nspanou@eagme.gr

Introduction

In light of the considerable impact of natural hazards on social, economic, and environmental stability, the comprehension of landslide phenomena represents a fundamental objective of scientific research. The utilisation of a landslide inventory enables the generation of susceptibility or hazard maps. In Europe, landslide inventories are accessible for numerous countries for national purposes, as well as in Greece (Dikau et al 1996, Eechhaut et al 2012, Hervás and Eechhaut 2013). It was deemed appropriate to ensure a representative distribution of events across Europe in order to facilitate the formulation of environmental policy and inform decision-making processes. This was due to the fact that landslides are considered to be one of the eight most significant soil threats in Europe (Gunther et al 2013). It is now well established from a variety of studies that the analysis of landslides supports the collection of existing data and the setting up of a Geographical Information System (GIS), enabling the creation of detailed geodatabases and maps.

The present study offers a comprehensive overview of the national-scale geodatabase of landslides in Greece. This database constitutes the most extensive source of information on landslides in Greece while it was compiled by the Hellenic Survey of Geology and Mineral Exploration (HSGME) following an extended period of documentation of landslide events across the country. The archive spans from the mid-20th century to the present day, continuously incorporating recent events. Currently, a dedicated Landslide Research Team is engaged in first-hand investigation of landslide occurrences, creating detailed reports that analyse the event's characteristics, causes, triggering factors, and consequences. These studies provide sufficient information for the specific characteristics as well as the evolution of landslides, which were then incorporated into the HSGME geodatabase.

Methods

The national landslide database was developed in accordance with the latest European policies and legislation. This geodatabase was constructed allowing the visualization of landslides' geometrical and geospatial features, as well as facilitating the statistical analysis of the data. The database itself is a relational management system meticulously compiled with over 5,500 individual landslide records, each studied in the field and aligned with European Union and United Nations directives on natural disaster risk mapping, fostering international collaboration in mitigating these threats (EC 2006). Access to the landslide geodatabase is currently available to various users within HSGME's local network and it will be made available to the general public via a web GIS platform in the near future. The geodatabase has been designed to accommodate multiple user access, allowing for concurrent or sequential access of different users, each with appropriate editing or reading rights. This configuration ensures immediate access and more rapid data modification, thus facilitating the collective scientific study of landslide phenomena. The geospatial data are organized into feature classes and tables, interconnected through specific relationships. These relationships correspond to information related to general ground failure elements (e.g., date of occurrence, location, source of information), geological elements (geotectonic and geotechnical units of landslide formations), causative factors, observed effects, protection measures, and more. This structure permits the incorporation of novel geodata, given the inherently dynamic nature of landslides, and guarantees the homogenization of the database through the verification and correction of existing records, including adjustments to the geospatial geometry of current entries.

Results

The formation of a landslide geodatabase provides the opportunity to digitize geospatial data into an incorporated and well-structured digital environment, whose structure is altered based on the user's requirements. The input data are classified, in order to ensure that landslide phenomena are tracked, analyzed, digitalized and presented geospatially, without any temporal limitations, opposed by the registration of a previous time, a lack of digital data, missing values, false correlations between past and present phenomena, as well as the false conclusions about landslide predictions. Based on the structure of the geodatabase, geospatial data offer the opportunity to users of also examining the relationship between landslide distribution and a range of causative factors including geological formations, topography, and hydrological characteristics. Moreover, the digitalization of landslide phenomena via the formation of the geodatabase, represents a new approach for public's awareness regarding landslides and natural hazards. Finally, the distribution of geospatial data, along with the potential for their further exploitation regarding future analysis and study, overcomes the past limitations of data mining and storage, given the instability of analogue data.

Conclusion

The improvement of the national landslide geodatabase marks a significant advancement in the analysis, management and mitigation of landslides in Greece. By digitalizing and structuring extensive geospatial and geological data, this database facilitates improved tracking, analysis, and visualization of landslide occurrences and their characteristics. The implementation of this geodatabase aligns with European policies and enhances accessibility and collaboration among users. Furthermore, this innovative approach not only aids in scientific research and hazard prevention but also promotes public awareness of natural hazards. As a crucial mitigation tool, the database's capability to integrate and analyze diverse data sets paves the way for more accurate predictions and well-informed decision-making, effectively addressing the limitations of previous data collection methods. The data and maps generated by HSGME also serve as a valuable tool for the Civil Protection Authorities.

References

Dikau, R.; Cavallin, A.; Jäger, S. Databases and GIS for landslide research in Europe. *Geomorphology*, 1996, 15, 3–4.

EC 2006 Thematic strategy for soil protection. COM (2006)231 final. Brussels: Commission of the European Communities.

Günther, A.; Reichenbach, P.; Malet, J.-P.; Van Den Eeckhaut, M.; Hervás, J.; Dashwood, C.; Guzzetti, F. Tier-based approaches for landslide susceptibility assessment in Europe. *Landslides*, 2013, 10: 529-546.Van Den Eeckhaut, M.; Hervás, J. State of the art of national landslide databases in Europe and their potential for hazard and risk assessment. Geomorphology, 2012,139–140, 545–558.

Hervás, J.; Van Den Eeckhaut, M. Landslide inventories in Europe and policy recommendations for their interoperability and harmonization, JRC, Publications Office, 2013.

CYCLONE DANIEL'S SCARS: A LANDSLIDE ANALYSIS IN METEORA, GREECE

NATALIA SPANOU[1], KATERINA KAVOURA[1], NIKOLAOS NIKOLAOU[1]

[1] *Hellenic Survey of Geology and Mineral Exploration, Greece;* nspanou@eagme.gr

Introduction

The severe weather event that occurred in September 2023, designated Cyclone Daniel, triggered extensive flooding and landslides across Central Greece. This event provides a unique case study for examining the link between extreme weather and landslide occurrences. This analysis focuses specifically on the Meteora municipality, an area in Greece that was heavily impacted by landslide phenomena triggered by Cyclone Daniel.

Methods

The detailed data on the Meteora landslide occurrences, triggered by Cyclone Daniel, has been subjected to meticulous in-situ investigation and subsequent analysis (Figure 1). The data set comprises information on the location, dimensions, and characteristics of the landslides. A total of 82 phenomena were documented within the municipal boundaries of Meteora. Landslide phenomena encompass a range of processes, including rotational and translational slides, as well as soil and debris flows. Erosions in stream beds are also a common occurrence. Finally, the accumulation of transported materials from the high steric supply of the streams is also a notable phenomenon.

The objective of this analysis is to ascertain the impact of the cyclone's intensity and precipitation patterns on slope stability within this region. Moreover, the efficacy of existing landslide susceptibility maps for the Meteora region has been evaluated. A comparison of these maps with the actual landslide distribution allows for an estimation of their effectiveness for the municipality and the identification of potential areas requiring adjustments.

Figure 1. A number of the impacts of landslides triggered by Cyclone Daniel in the Meteora region.

Results

This study aimed to decipher the mechanisms that precipitate landslides in the Meteora municipality, which was significantly impacted by Cyclone Daniel. The particular meteorological factors that trigger landslide events within the municipality have been identified. Additionally, the accuracy of existing susceptibility maps in predicting landslide locations during extreme weather events has been assessed. Finally, recommendations for enhanced landslide risk mitigation strategies that are specific to Meteora and have potential applicability to other vulnerable municipalities have been put forth.

Conclusion

Following the conclusion of this study, the most effective protection and mitigation measures were identified as surface water settlement projects, underground water drainage, and, in the case of landslides, a case-by-case approach for the selection of appropriate support works. Additionally, demarcation studies must be conducted to identify and delineate the areas that have been affected or are at risk of being affected. Finally, the maintenance and repair of infrastructure along the road network is essential to ensure the continued functionality and safety of the transport infrastructure, including technical components, bridges and other structures.

Acknowledgements

This study was conducted utilizing the "Landslide Susceptibility Map of Greece," which was developed within the framework of the Operational Program entitled "Competitiveness, Entrepreneurship and Innovation (2015-2020), Project “Studies and researches support to the energy sector, industry and entrepreneurship”, Sub-Project “Susceptibility assessment of landslides in the Greek territory - Volcanic study and risk assessment”, financed by the European Regional Development Fund.

LANDSLIDE MAPPING AND MODEL DEVELOPMENT FROM MULTI-LEVEL REMOTE SENSING TECHNOLOGIES DATA, HRVATSKA KOSTAJNICA CASE STUDY, CROATIA

IVAN KOSOVIĆ[1], LASZLO PODOLSZKI[1], TOMISLAV NOVOSEL[1], TOMISLAV KUREČIĆ[1]

[1] *Croatian Geological Survey, Sachsova 2, Zagreb, Croatia; corresponding author: ikosovic@hgi-cgs.h*

Introduction

Geohazards are a constant threat to human activity in an environment that is constantly changing. Climate changes affect the natural extremes, resulting in rapid temperature changes, flooding, and a high amount of precipitation in a short period. Furthermore, landslides can have several causes, including geological, morphological, physical, and human factors (Alexander 1992). However, they typically have only one trigger. This trigger can often be intense rainfall, earthquake shaking, storm waves, or rapid stream erosion (Varnes 1978). Such unpredictable events can affect slope stability, leading to new landslides and the reactivation of old ones. Predicting the behavior of soil and rock masses during and after extreme events is a crucial yet complex task. Different remote sensing technologies calibrated through local scale datasets can be used and integrated to enhance the knowledge and understanding of the event.

After a rapid temperature change and snowmelt on March 13, 2018, a landslide in Hrvatska Kostajnica destroyed multiple households. The Hrvatska Kostajnica landslide case study introduced a new integrated approach to geohazard research. The research utilized various multi-level remote sensing techniques, and the results were analyzed and integrated to develop a comprehensive landslide model.

Methods

Approaches used in this research included the review of available datasets and the acquisition of new data to develop a landslide model. The new datasets included: 1) remote sensing data, 2) field research, and 3) laboratory data with associated analysis and re-interpretation. The main focus was on acquiring multi-level remote sensing technologies and data such as orthophoto data, unmanned aerial vehicle (UAV) data (Ngadiman et al., 2016), differential interferometric synthetic aperture radar (DInSAR) data (Ferretti et al., 2007), light detection and ranging (LIDAR) data (Jaboyedoff at al., 2012), and geophysical measurements, i.e., electrical resistivity tomography (ERT) data (Loke et al., 2013).

Results

The landslide in Hrvatska Kostajnica covers an area of approximately 300 × 300 m with a maximum height difference of about 60 m (Figure 1). The developed 26 m high detailed geological column at the main scarp revealed that the landslide occurred mainly in the "marly" sediments. Clayey (weathered) limestones were also present at the location, but no clear sliding zone(s) were mapped on the field during geological column development.

The DInSAR data analysis was used in surface displacement behavior trend determination and it indicated that the landslide was a "short and extreme" event rather than a long-term, ongoing, slow slope deformation process. ERT was applied to determine the physical properties of soil and rock, subsurface lithology, groundwater conditions, and geometry of the slide surface. The cross sections within the landslide body (ERT-1 and ERT-2) revealed zones with colluvial materials, in the range of 5–20 Ωm. Below colluvial materials, weathered and interlayered materials are present (with resistivity values in the range of 20–50 Ωm). The "bedrock" on the ERT-1 and ERT-2 is probably a heterogeneous structure (interlayered materials), but not so weathered and with somewhat higher resistivity values (>50 Ωm).

From the available regional data, the area is generally prone to landslides (Podolszki et al., 2022). The preliminary landslide model indicated an affected area of approximately 5 ha with multiple sliding surfaces, the deepest at around 30 m. The multiple datasets acquired in the scope of this research (UAV, DInSAR, LIDAR, and ERT data) and historical orthophotos provided different useful insights that were collectively used to develop a new model of the landslide. ERT results showed that the landslide has multiple sliding surfaces and that highly deformed materials are present mainly in the main body of the landslide. The sliding surfaces within the landslide body are at depths of around 10–20 m. Additionally, the model identifies a relatively large landslide-endangered zone of approximately 12.5 ha. Based on the characteristics of this particular event (deep-seated with multiple sliding zones) and the collected data, it can be assumed that the the triggering factor was the contemporaneous rapid temperature change driving a sudden snowmelt (~80 cm of snow cover melted) and the Una River flooding (located ~400 m from the landslide and showing a water level ~5 m higher level than usual during the flooding event). These factors probably increased the water pore pressure in the rock mass and the rhythmic changes within the material caused multiple weakened zones. Despite the potential influence of anthropogenic factors in triggering landslides, human activities played little to no role in this instance.

Figure 1. Hrvatska Kostajnica landslide location: A) In the city of Hrvatska Kostajnica near Una River; B) In Croatia, near the border with Bosnia and Herzegovina (red mark on the map)

Conclusion

Field mapping and UAV data collection were performed for the revision of available geological and remote sensing data of the Hrvatska Kostajnica landslide. A new geological column was developed and available remote sensing data were analyzed, namely satellite images and historical orthophotos. New insights about the Hrvatska Kostajnica landslide were gained by LIDAR and geophysical data analysis. From detailed LIDAR data, a precise terrain landslide surface model was developed and used for the cross-section and new landslide map development. These data allowed us to propose a new model of the landslide showing a potential endangered area larger than the area predicted by a preliminary model.

References

Alexander, D. 1992. On the Causes of Landslides: Human Activities, Perception, and Natural Processes. *Environmental Geology and Water Sciences*, Vol. 20, No. 3, pp. 165-1 79.

Ferretti, A.; Monti-Guarnieri, A.; Prati, C.; Rocca, F.; Massonnet, D. InSAR Principles: Guidelines for SAR Interferometry Processing and Interpretation; *ESA Publications*: Auckland, NZ, USA, 2007; ISBN 92-9092-233-8.

Jaboyedoff, M.; Oppikofer, T.; Abellán, A.; Derron, M.H.; Loye, A.; Metzger, R.; Pedrazzini, A. Use of LIDAR in landslide investigations: A review. *Nat. Hazards* 2012, 61, 5–28.

Loke, M.H.; Chambers, J.E.; Rucker, D.F.; Kuras, O.; Wilkinson, P.B. Recent developments in the direct-current geoelectrical imaging method. *J. Appl. Geophys*. 2013, 95, 135–156.

Ngadiman, N.; Kaamin, M.; Sahat, S.; Mokhtar, M.; Ahmad, N.F.A.; Kadir, A.A.; Razali, S.N.M. Production of orthophoto map using UAV photogrammetry: A case study in UTHM Pagoh campus. In *AIP Conference Proceedings*; American Institute of Physics: College Park, ML, USA, 2016.

Podolszki, L.; Kosović, I.; Novosel, T.; Kurečić, T. Multi-Level Sensing Technologies in Landslide Research — Hrvatska Kostajnica Case Study, Croatia. *Sensors*, 22 (2022), 1; 177, 21.

Varnes, D.J. 1978. Slope Movement Types and Processes. *In Special Report 176: Landslides: Analysis and Control* (R.L. Schuster and R.J. Krizek, eds.), TRB, National Research Council, Washington, D.C., pp.12-33.

ASSESSING ROCKFALL HAZARDS POST-WILDFIRES: A CASE STUDY IN EVROS, GREECE

PAVLOS ASTERIOU [1], DIMITRIS SOTIRIADIS [2], ELENI PETALA [3], LABROS KAZELIS [4], EVAGGELOS EVAGGELOU [5], THEOFILOS TZEVELEKIS [6], NIKOS KLIMIS [7]

[1] *Democritus University of Thrace, Department of Civil Engineering, Greece,* pasterio@civil.duth.gr

[2] *Democritus University of Thrace, Department of Civil Engineering, Greece,* dsotiria@civil.duth.gr

[3] *Democritus University of Thrace, Department of Civil Engineering, Greece,* epetala@civil.duth.gr

[4] *Democritus University of Thrace, Department of Civil Engineering, Greece,* labrkaze@civil.duth.gr

[5] *Democritus University of Thrace, Department of Civil Engineering, Greece,* eevange@civil.duth.gr

[6] *Democritus University of Thrace, Department of Civil Engineering, Greece,* thtzebel@civil.duth.gr

[7] *Democritus University of Thrace, Department of Civil Engineering, Greece,* nklimis@civil.duth.gr

Introduction

Following wildfires, rockfalls in forested slopes are expected to increase in occurrence, frequency, and severity, posing a greater hazard to mountainous settlements and infrastructure. Vegetation typically mitigates rockfalls by restricting block movement and absorbing energy through collisions with tree trunks. However, the destruction of vegetation negates this beneficial action, resulting in extended run-out distances and intensified impacts. Moreover, the temperature rise during a wildfire may degrade rock properties, potentially reducing their resistance and increasing the number of unstable blocks. As a result, both the likelihood and consequences of rockfall events, namely the hazard, may heighten. In this paper, we examine these parameters in the Avas site, located in Regional Unit of Evros, Greece, that was heavily impacted by the 2023 wildfire. Figures 1 (a) and (b) illustrates the study area before and after the wildfire, respictevely. The fire started on August 21st, 2023, and burnt more than 800km^2, making it the largest wildfire ever recorded in the EU.

Methods

We deployed to the field to gather all necessary information, including Schmidt hammer hardness, vegetation type, size and density and identified the size and location of previously detached blocks. Then, we composed the geological and vegetation maps of the site. Along with the 2-meter resolution Hellenic Cadastre raster map, we analysed the possible rockfall trajectories in the three-dimensional space using the RockyFor3D (Dorren, 2016) software to evaluate the effect of vegetation. We examined two scenarios: the first with the site's vegetation before the fire, and the second without any vegetation to simulate its destruction after the fire. For each scenario, we analysed cubic blocks with volumes of 1m^3, 0.1m^3 and 0.01m^3, released from the top of the slope. In each analysis, we released 10 blocks from every cell, resulting to a total of 6590 blocks. The vegetation of the study area was measured in patches that remained unburnt. It consists of small Mediterranean scrublands, with a mean density of 6875 stems per hectare and an average stem diameter of less than 5 cm.

Results

First, the findings indicated that the temperature rise did not influence the rock properties, as Schmidt hardness values were similar for both burnt and unburnt rock exposures. This is supported by the fact that even though the branches and leaves of the trees were completely burnt, their stems were only superficially burnt, indicating that the fire passed through the site quickly, resulting in a moderate temperature rise. The analyses with the 1m^3 blocks had similar results to the 0.1m^3 blocks and are not presented hereafter. This is attributed to the fact that this vegetation type has limited capacity to withstand impacts, thus having a limited effect on blocks larger than 0.1m^3. This is in line with Figure 1 (c) and (d), which presents the end positions of the 0.1m^3 blocks in the forested and burnt scenarios, respectively, where the effect of vegetation is negligible. However, when examining Figure 1 (c) and (e), it is seen that smaller blocks travel less. This is attributed to two reasons: first, larger blocks tend travel longer distances as they are less affected by the irregularities of the slope (Ritchie, 1964 and others), and second, this type of vegetation is more effective in restricting blocks with less energy. For the 0.01m^3 blocks, the destruction of vegetation increases the hazard (Figure 1 (e) and (f)), as more blocks impact the road, especially on its south side.

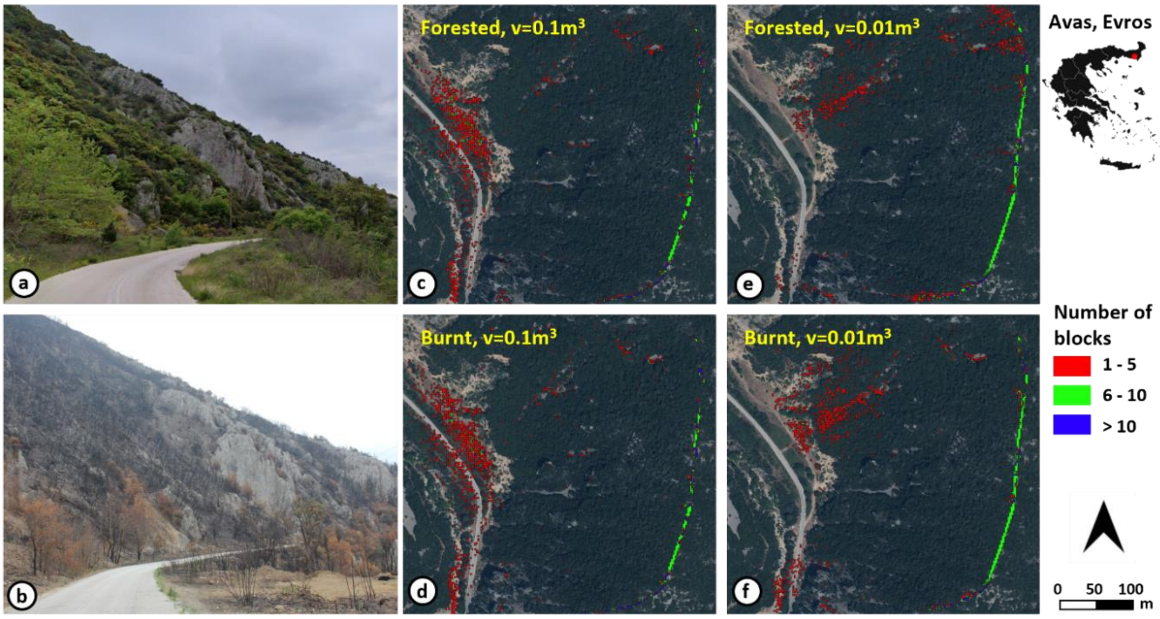

Figure 1. Avas site, (a) before and (b) after the wildfire. Trajectory end points: (c) Forested slope with v=0.1m^3, (d) Burnt slope with v=0.1m^3, (e) Forested slope with v=0.01m^3 and (f) Burnt slope with v=0.01m^3,

Conclusion

The destruction of vegetation due to wildfires increases rockfall hazard as the blocks tend to travel further down the slope. The vegetation type plays a significant role; in Avas study area, the vegetation was weak, primarily affecting small-sized blocks. However, in areas with stronger vegetation, the increase in hazard will be more pronounced for larger blocks. On the other hand, we did not find any evidence that the rock properties degraded from the wildfire in Avas study area.

Following wildfires, various measures are often taken to mitigate the destructive effects of phenomena such as floods, landslides, and others. Although rockfalls may evolve gradually, it is crucial to promptly acknowledge their increased threat. By doing so, rockfall mitigation efforts can be integrated with other early interventions aimed at addressing different consequences. This integrated approach enables a more efficient management of the necessary actions, resulting in cost savings and, ultimately, to the restoration of safety levels to acceptable standards.

Acknowledgement

This project (KE83226) was funded by Democritus University of Thrace under the initiative “DUTh To The People: Actions to Mitigate the Effects of the Devastating Fires in Thrace.”

References

Dorren, L.K.A. *Rockyfor3D (v5.2) revealed – Transparent description of the complete 3D rockfall model*. ecorisQ paper (www.ecorisq.org), 2016.

Ritchie, A. M. *Evaluation of rockfall and its control*. Highway research record 17, pp. 13-28, Washington, USA, 1963.

STREAMLINING ROCKFALL ANALYSIS: A DIGITAL PARADIGM FOR EFFICIENCY, COLLABORATION AND RISK MANAGEMENT

ALKIS GKOUVAILAS [1], İREM AKSULAR [2], S.W.R CHAN [3], H.L.K FU[4], FINLAY LEIBRICK[5]

[1] *Langan Engineering and Environmental Services, United Kingdom,* agkouvailas@langan.com

[2] *AECOM, UAE,* irem.aksular@aecom.com

[3] *AECOM, UAE,* swrachael.chan@aecom.com

[4] *AECOM, Hong Kong,* karen.fu@aecom.com

[5] *AECOM, UAE,* finlay.leibrick@aecom.com

Introduction

Mountains in the Middle East have great geo-heritage value due to their intriguing geological setting. The region envisions leveraging its endowed natural beauty for ecotourism and development, leading to a growing need for rock slope stability and rockfall studies. Given the complexity and scale of projects, combined with their expeditious time frame, it is crucial to carry out these studies efficiently to inform project risk assessment and decision-making for mitigation and master planning in a timely manner.

This paper presents a streamlined workflow for rockfall analysis employed in a recent project close to Riyadh, Kingdom of Saudi Arabia, which successfully achieved the goals outlined above. The proposed development will be situated within a vast landscape featuring desert, plateau, mesas and butte, with encircling cliffs reaching heights of 200 m and spanning over 15 km. This expansive terrain has exhibited signs of historic rock slope instabilities, necessitating detailed geological and geohazard assessments with a focus on rockfall risks. To perform such a comprehensive engineering geological study, an ArcGIS-based paradigm furthering the work of Charalambous and Sakellariou (2007) was implemented, following the workflow shown in **Figure 1Figure 1**.

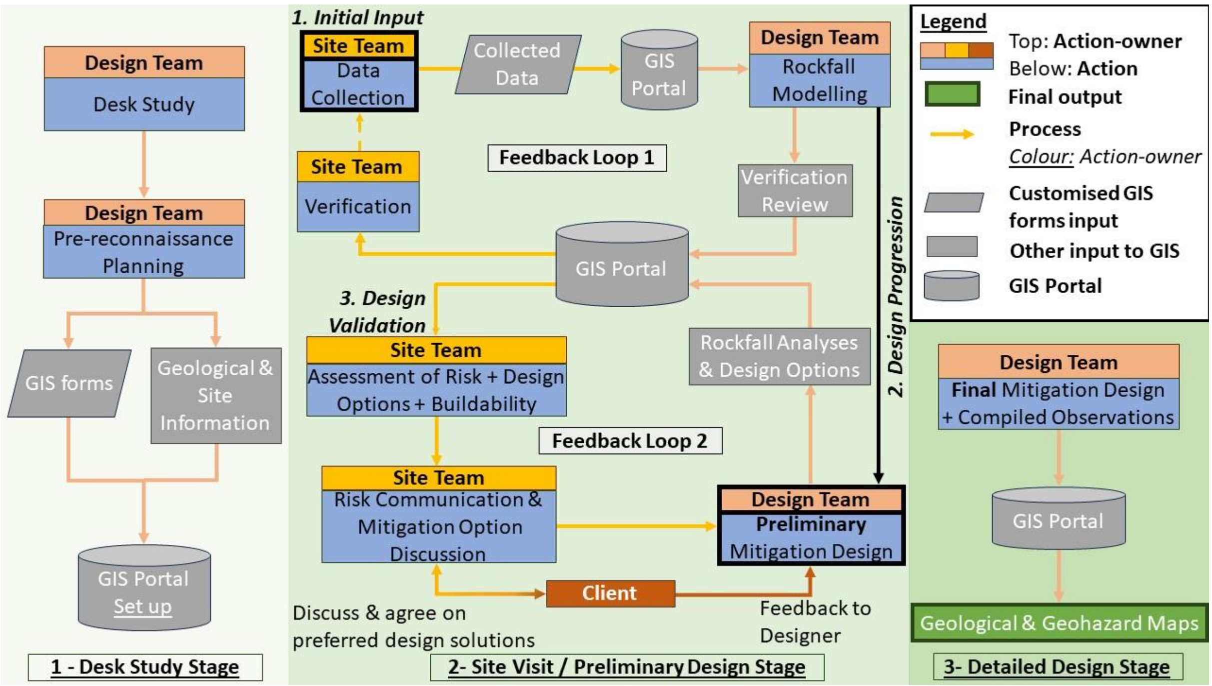

Figure 1. Presented digitalised workflow for rockfall analysis.

Methods

To ensure a focused survey and to develop a better understanding of the site geology and ground conditions, a desk study was carried out through a review of available information. Earlier mapped geological boundaries and features, slope angle and plot boundary were compiled on ArcGIS for the identification of critical rockfall areas and the formulation of visit routes. The acquired information was pre-loaded through the ArcGIS Online portal, into the ArcGIS Field Map application to be available for offline usage onsite. Moreover, project-specific observation forms were built through ArcGIS Field Map Designers for an expedited and standardised data collection process. These forms, informed by insights from past projects and client feedback, were configured for direct import into rockfall analysis software.

Site data from the geological and geohazard mapping was captured on ArcGIS Field Map, along with geotagged photos for subsequent evaluation. These included observations of geological boundaries, engineering-geological descriptions of soil and rock, and geohazards. Furthermore, an online inventory of historical rockfalls and susceptible areas was integrated as part of the geohazard mapping. It entailed details like originating, impact and termination points, rock block dimensions and shapes, and observed failure mechanisms. All data collected was georeferenced and stored in one central database via the ArcGIS Online portal for usage across different ArcGIS platforms. The integrated acquisition approach allowed the collected data to be shared seamlessly with office designers, enabling the design team to swiftly review it and raise queries or verification requests with the site team while they were still onsite.

In parallel with the field work, designers performed rockfall analysis. Given the terrain complexity, three-dimensional (3D) rockfall modelling was employed through RocFall3®. Input parameters (i.e., coefficients of restitution) were initially assessed based on literature (Gkouvailas, 2014) and then adjusted through back analysis. This was made possible by the streamlined data collection process through which a detailed historical rockfall database was produced. Once the models effectively replicated the historical rockfall events, a series of originating points were placed at all potential initiation locations. Two-dimensional (2D) analyses through RocFall2® were undertaken for critical rockfall trajectories to inform the design of mitigation measures. To facilitate the identification of critical areas and risk assessment, the trajectories were overlaid onto the master plan in the GIS model through a self-developed GIS toolbox. The project site was divided into zones so that rockfall models could be constructed in parallel with the site work. The analysis results (trajectories, kinetic energies, etc.) for the previously mapped areas were shared via the GIS portal with the site team, which enabled real-time validation onsite. Feasibility and applicability of the proposed mitigation were evaluated in the field.

Remote sensing data was utilised to supplement the geological assessment and combined with site observations and rockfall models to create geological and geohazard maps for the project area. Identified risks, their locations and analysis results were incorporated into the project's risk registry. Risks and mitigation measures were communicated to and discussed with the client onsite with the aid of graphics and 3D models to visualise the impact on master planning. This allowed engaged and informed decision-making from the client’s side and provided prompt feedback to the design team.

Results and Conclusion

This digitalised strategy reduced time on site and subsequent data processing. The planned visit with tailored GIS tools promoted targeted surveys with integrative outputs to be fed into rockfall analysis and geological/geohazard mapping. The simultaneity of observation and backend analysis increased the comprehensiveness of inspection and modelling accuracy and improved design efficiency and quality. Additionally, timely, direct, and continuous communication with the client on the site findings, identified geohazards and mitigation solutions optimised the design process and overall project risk management. Considering the proven benefits, this rockfall study blueprint is encouraged for future use.

References

Charalambous, S.; Sakellariou, M. Estimation of rockfall hazard using a GIS-based three-dimensional rockfall simulation model. *Bulletin of the Geological Society of Greece*. 2007, 40 (4), 1934-1946

Gkouvailas, A. Enhanced rockfall analysis based on field experiments in quarries in the UK. *Master Thesis, Imperial College London*, UK, 2014.

Geomorphic effectiveness of flood discharge and its importance for river-bed engineering constructions: a case of the Godavari, India

SUMIT DAS [1], GIANVITO SCARINGI [1]

[1] *Institute of Hydrogeology, Engineering Geology and Applied Geophysics, Charles University, Czech Republic, sumit.das@natur.cuni.cz, gianvito.scaringi@natur.cuni.cz*

Introduction

Floods are a frequent and devastating natural disaster that affects many regions worldwide. While they cannot be fully prevented, adopting suitable strategies can mitigate their geomorphic impact and severity. This is especially true for engineering riverbed constructions in populous areas. Systematic assessments of flood intensity are crucial for effective flood management (Cameron et al., 2000). The impact of a major flood is determined by various factors including the flow's strength, the energy of the stream, the sequence of events, and the shape of the river channel (Miller, 1990; Das 2019). Riverbed constructions such as bridges significantly affect the river's cross-sectional morphology and, therefore, the flood effectiveness. Here, we study the geomorphic impact of floods under typical conditions using a theoretical framework and examine how bridges affect flood dynamics.

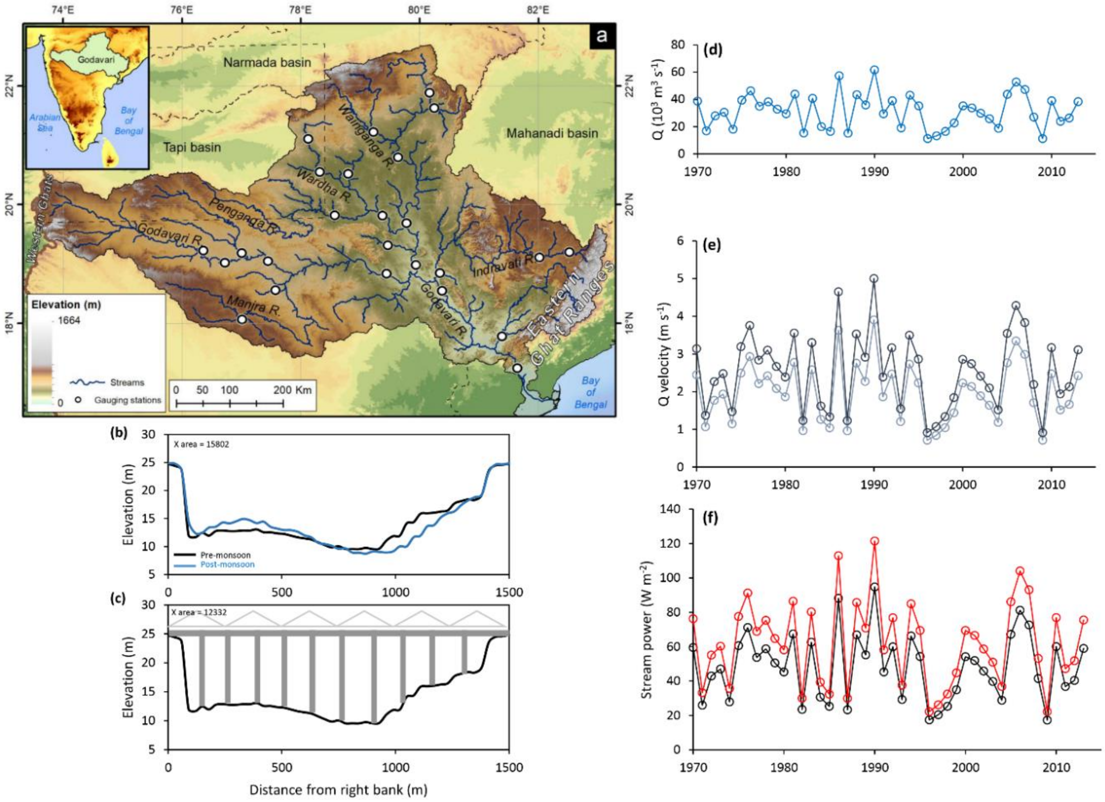

Figure 1. (a) Map of the Godavari basin. (b) Polavaram's river cross-section on the Godavari, and (c) the same section assumed with a bridge comprising 10 pillars of 5 m radius, reducing the area from 15,802 to 12,332 m^2. (d) Yearly fluctuation of peak discharge at Polavaram; (e) changes in peak discharge velocity under normal conditions and with a bridge; (f) stream power variations for both scenarios (black: normal; red: bridge).

Study area and methods

The Godavari basin in Peninsular India has the largest catchment area in the region, spanning over 300,000 km^2 (Fig. 1a). Its rivers flow through three major lithological zones: Deccan basalt in the west, Precambrian Gondwana sedimentary rocks (including sandstone and shale) in the centre, and Archean granite and gneiss in the east. Additionally, the delta region features extensive Quaternary alluvium deposits mixed with moderate-sized gravel and sand.

In this work, ranging from 1970 to 2015, we gathered long-term discharge data and historical cross-sectional measurements for various gauging stations of the Godavari River from the Central Water Commission (CWC), India. We calculated cross-sectional morphology parameters, namely width, mean depth, area, width-depth ratio, hydraulic radius, and shear stress (τ). We then identified the peak annual

discharge as the effective flood for each year to determine the unit stream power (ω) (Leopold et al., 1964). Considering the principle of discharge continuity, we recalculated all parameters under the hypothetical scenario of a bridge being constructed at each cross-section (Fig. 1b & c). This would lead to a notable decrease in cross-sectional area. Given that discharge remains constant across a channel section (theoretically, unless joined by a new tributary), the flood discharge must adjust its flow velocity accordingly. Using historical flood discharge data, we calculated velocities for both standard conditions and with a hypothetical bridge in place, followed by unit stream power computations.
Subsequently, we applied William's (1983) equation to estimate the entrainment potential of various boulder sizes based on the calculated flood stream power in both scenarios. This method's significance lies in evaluating the impact of engineering structures on riverbeds, determining their safety against high floods, and assessing whether such constructions could be severely impacted by flooding.

Results

Our calculations are based on the assumption that the annual peak discharge equates to the bank-full stage for ease of analysis. However, real-world scenarios may differ from this theoretical model. Nevertheless, Table 1 illustrates the cross-sectional parameters for the Polavaram station on the Godavari River. The flood discharge has been recorded ranging from 11×10^3 m^3 s^{-1} in 2009 to an unprecedented 62×10^3 m^3 s^{-1} in 1990, as depicted in Fig. 1d.

Table 1. Computational results of the cross-section geometry and hydraulics.

Parameters	Value
Width (m)	1500
Average depth (m)	10.33
Area (m^2)	15802
Form ratio (Width/Depth)	145.22
Slope (degree)	0.00024
Manning's n	0.024
Boundary shear stress (N m^{-2})	24.29

The terminal gauging station of the Godavari at Polavaram spans 1500 m in width, with maximum and average depths of 15.26 m and 10.33 m, respectively. In evaluating the river cross-sections to understand the flow behaviour, the computed boundary shear stress at this site is 24.29 N m^{-2}. Manning's "n" value, determined by observing channel roughness, bed material, and land use, is 0.024. Under standard conditions, the unit stream power is observed to vary from 17 to 94 W m^{-2}. However, when we simulate the construction of a bridge with 10 pillars, each 5 m in diameter, the stream power increases to 22 to 121 W m^{-2} (Fig. 1f), and the cross-sectional area decreases from 15,802 to 12,332 m^2 (Table 1), assuming a fixed cross-section. In reality, extreme floods can alter cross-sections significantly, and regular assessments of stream power are vital for areas upstream and downstream of dam constructions to prevent potential flood damage to engineering structures and minimize risks to flood-prone areas.

Conclusion

This study offers a theoretical evaluation of flood dynamics in the Godavari River, which is instrumental in safeguarding engineering structures from flood damage and implementing effective flood mitigation strategies for the adjacent areas.

References

Cameron, D.; Beven, K.; Naden, P. *Flood frequency estimation by continuous simulation under climate change (with uncertainty)*. Hydrol. Earth Syst. Sci. 2000, 4, 393–405.
Das, S. *Geospatial mapping of flood susceptibility and hydro-geomorphic response to the floods in Ulhas basin, India*. Remote Sens. App. Soc. Env. 2019, 14, 60-74.
Leopold, L.B.; Wolman, M.G.; Miler, J.P. *Fluvial Processes in Geomorphology*. Freeman, San Francisco, 1964.
Miller, A.J. *Flood hydrology and geomorphic effectiveness in the central Appalachians*. Earth Surf. Process. Landf. 1990, 15, 119–134.
Williams, G.P., *Paleohydrological methods and some examples from Swedish fluvial environments: I. Cobble and boulder deposits*. Geogr. Ann. 1983, 65A, 227–243.

MINING-INDUCED SUBSIDENCE SUSCEPTIBILITY MODELLING OF THE WITWATERSRAND BASIN USING WEIGHTS OF EVIDENCE (WOE) APPROACH IN GIS

S.G. CHILIZA[1], N. MANKAYI[1], M. SEBESHO[1], C. GABAVANA[1], AND G DENNER[1]

[1.] *Council for Geoscience, 280 Pretoria Road, Silverton, Pretoria, 0184, South Africa, msebesho@geoscience.org.za*

Introduction

Mining activities in South Africa have altered the natural environment in numerous ways over the last 120 years. Areas within the Witwatersrand basin located in Johannesburg, Gauteng's East, West Rand and Far West Rand districts, including the KOSH (Klerksdorp-Orkney-Stilfontein-Hartebeesfontein) mining regions, are subjected to ground settlement and surface subsidence due to mining (historical, and current illegal mining) and groundwater dewatering for mining operations to take place (Heath and Engelbrecht, 2011). In response, the Council for Geoscience (CGS) embarked on research seeking to produce land subsidence susceptibility maps that will categorise the abandoned mine areas into zones with varying degrees of subsidence susceptibility driven by previous subsidence inventory data and contributing factors that will aid spatial planning decision making and disaster management.

Methodology

The weight-of-evidence (WoE) statistical approach was selected and used for subsidence susceptibility mapping (Oh & Lee, 2010). This approach computes the conditional probability that an event (in our case, mining-induced subsidence) does or does not belong to a set of mapped causal factors (i.e., conditioning factors). Physical processes known to occur in gold mining settings and the historical perspective of the study area were used to select potential conditioning factors. The WoE theoretical framework was then implemented to objectively assess the relevance of these conditioning and triggering factors.

Broadly, the following steps were completed:

1. Establishment of a comprehensive database/inventory of mining-induced subsidence events (including dewatering for mining).
2. Determination of potential conditioning factors based on geological processes inferred: Proposed conditioning factors were slope, geology, groundwater (dewatered and non-dewatered compartments), faults, and mined-out areas.
3. A probabilistic WoE evaluation of the potential conditioning factors followed by a test of independence of conditioning factors
4. Developing a susceptibility map by combining relevant conditioning factors and validating the map with receiver operating characteristic (ROC) curves.

Results

The results show that groundwater in the form of de-watering has the highest influence on subsidence, with the highest contrast (C value) of 2.33. The geology (dolomitic formations), slope, faults, shaft positions and mined-out areas were found to have weights of 2.08, 1.49, 0.37, 0.63 and 0.42, respectively. The dewatering of Venterspost, Oberholzer, Bank, and Gemsbok-west to allow mining operations has led to the accelerated sinkhole and subsidence occurrences on the Far West Rand, and approximately 1200 events have occurred to date. The mining-induced subsidence susceptibility map for the Far West, West, Central and East Rands of the Witwatersrand goldfields basin is shown in Figure 1. From this map, the analysis of results shows that the actual ground subsidence is in high and very high subsidence susceptibility areas, as confirmed by the AUC method.

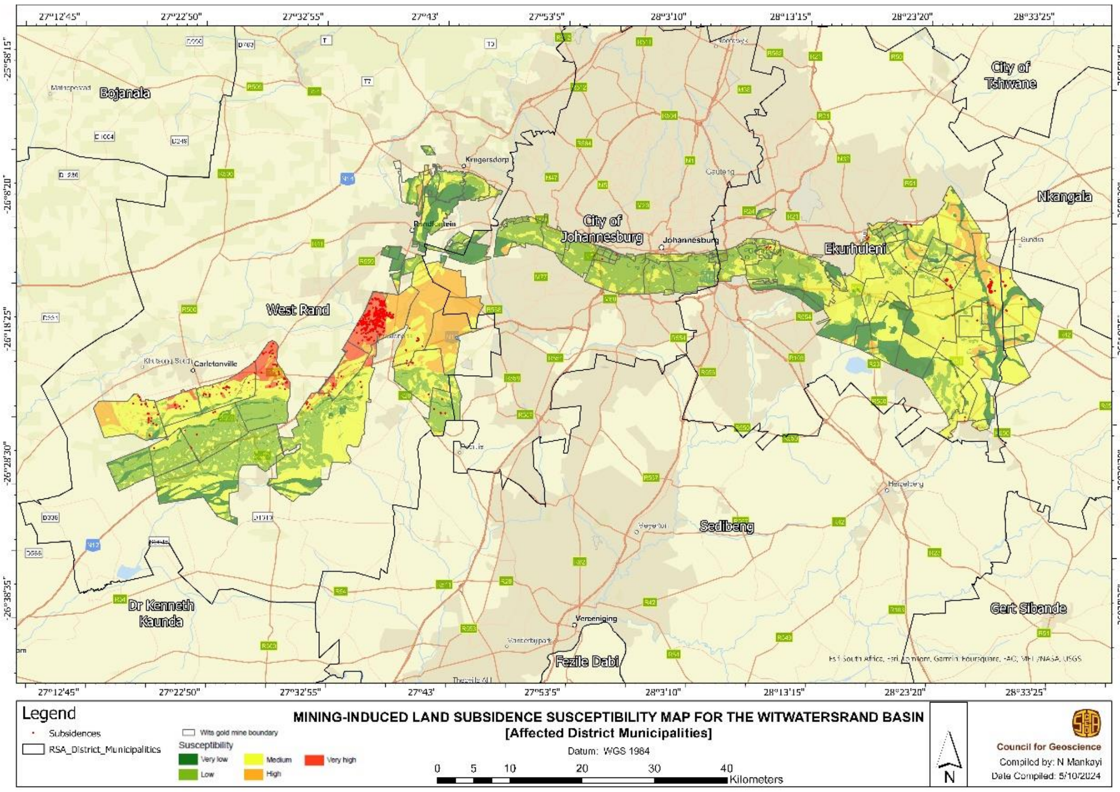

Figure 1: Mining-induced subsidence susceptibility map the Witwatersrand Basin.

Conclusions

The dewatering of dolomite groundwater compartments for mining has been highlighted as the major contributor to the formation of sinkholes and subsidence in the West and Far West Rand areas of the Witwatersrand basin. Therefore, the results presented here must inform future policy and decision-making around dewatering for mining. Given the knowledge, experience and susceptibility modelling results, it is therefore concluded that most of the resources and efforts for monitoring subsidence must be deployed in the Central Rand and parts of the West and East Rands and at all illegal mining hotspots.

References

Heath, H. and Engelbrecht, J. Deformation due to mining activities. Council for Geoscience Internal Report No: 2011-065, 2011

Oh, H. and Lee, S. Assessment of ground subsidence using GIS and the weights-of-evidence model. Engineering Geology, Volume 115, 2010, pp. 36-48.

FOLD-CONTROLLED ROCK SLIDING DETERMINED FROM STRUCTURE AND 2D INSAR PRESENTS A LOW HAZARD: THE CASE OF DUSNJÁRGA, NORTHERN NORWAY

LOUISE M VICK[1], ANDREAS GRUMSTAD[2], CARLY FABER[3], LINE ROUYET[4], SIMEN BEKKEVOLL[5]

[1] *UiT The Arctic University of Norway, Norway, louise.m.vick@uit.no*

[2] *UiT The Arctic University of Norway, Norway, andreas.grumstad@uit.no*

[3] *UiT The Arctic University of Norway, Norway, carly.faber@uit.no*

[4] *NORCE, Norwegian Research Center, Norway, liro@norce.no*

[5] *Troms Fylkeskommune, Norway, simen.bekkevoll@tromsfylke.no*

Introduction

Dusnjárga is a large deforming rock slope in the Kvænangen area of northern Norway. It sits on a peninsular in the Little Altafjord, framed by a series of rock slope deformations (RSD) (Figure 1). These RSD pose a threat to surrounding seaside villages from collapse and tsunami, should they fail. RSDs can creep for up to thousands of years before collapse (McColl & Draebing, 2019), and in some cases may stabilise rather than fail at the end of the creep phase. In remote and alpine cases it is not possible to drill for subsurface information and therefore an interpretation of the mechanics must be made from the surface data. In this work we employ structural data combined with movement from 2D InSAR to assess the kinematics of Dusnjárga to assess the hazard potential of the site.

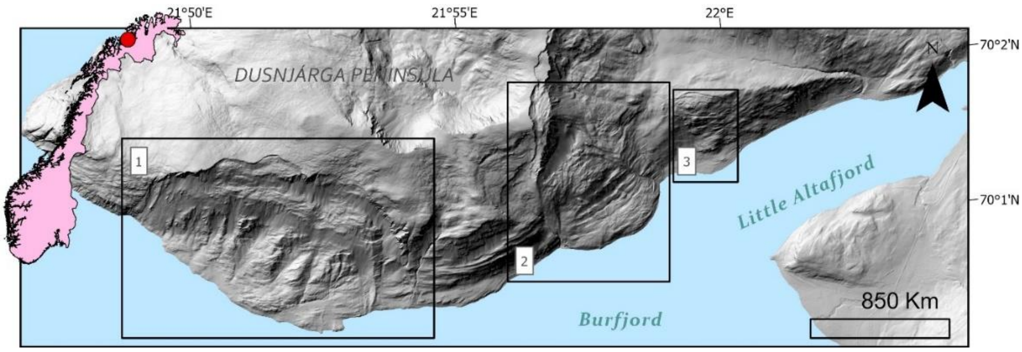

Figure 1. Location map. 1.Vassnestinden RSD, 2. Dusnjárga RSD, 3. Låvan RSD. Inset map with red dot shows generalised location of study area. DEM 2016 series from hødedata.no, sampled at 1m resolution.

Methods

Structural data was collected during summer campaigns in 2019-2021. >3000 structural observations were made, mostly with the FieldMOVE app. InSAR data used in this thesis comes from the public service *InSAR Norway* 2015-19 Copernicus Sentinel-1A and -1B satellite data. 2D InSAR interpolates displacement from two radar geometries to harvest a vector within a profile line (e.g. Frattini et al., 2018). A GIS tool (Lauknes et al., 2020) was used to combine data from overlapping SAR imagery to estimate a combined annual mean velocity. The stable plateau above was used for calibration.

Results

The RSD has a clearly defined detachment limit and coastline toe-bulge, with many scarps and areas of dense fracturing and talus. The slope is comprised of metagrabbro and amphibolite, displaying a range of foliations from weak to strongly pervasive. Some parts of the metagabbro are mylonitised with an intensely planar fabric. The foliation in general dips downslope between 800-150 m asl. Below 150 m, it appears to dip into the slope (Figure 2). The pattern of foliation indicates a large synclinal structure may be present. This is congruent with the displacement vector dip (Figure 2), which shows a movement of the slope downwards from 800 m until ca. 150 m asl, where the slope surface begins to move up and outwards, potentially by slippage along structures associated with the fold.

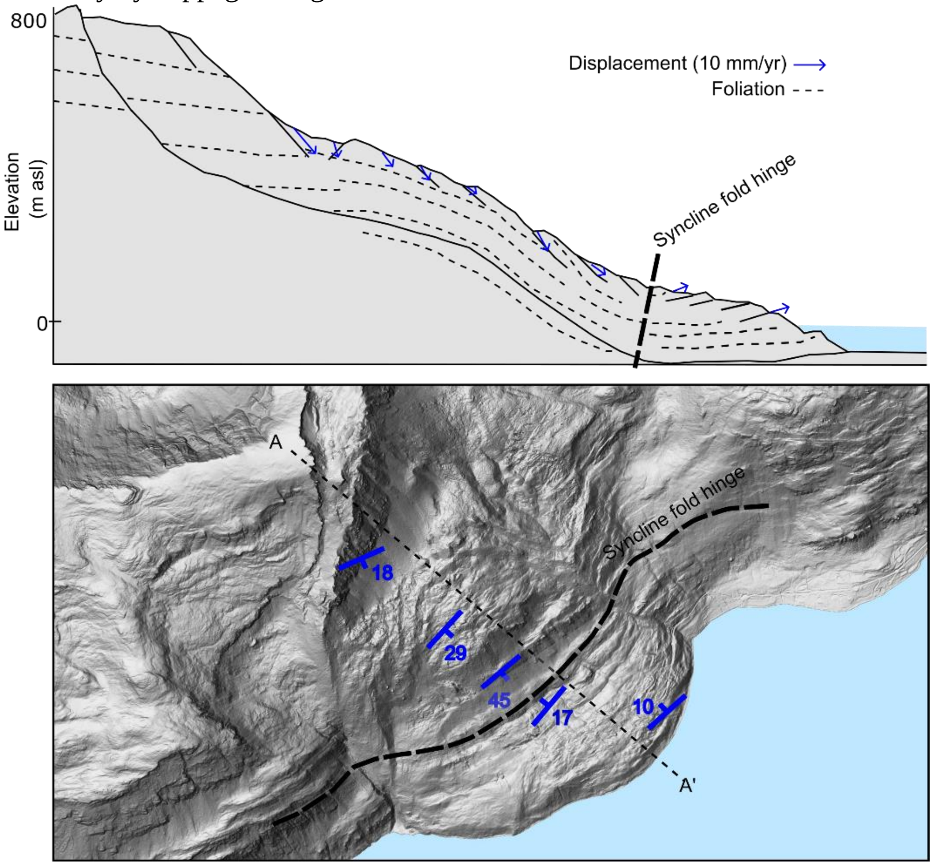

Figure 2. Upper panel: Cross section showing surface morphology, inferred foliation and surface displacement vectors. Lower panel: multiaspect hillshade (from 1 m DEM) showing foliation dip and direction and syncline surface trace.

Conclusion

The combination of structural mapping and 2D InSAR provides insight into the mechanical model of the Dusnjárga RSD. If the basal sliding surface is controlled by a syncline structure, a buckling-style failure (Glastonbury & Fell, 2010) must be considered where friction at the toe cannot be overcome, and transported material becomes imbricated at the toe, after e.g. Braathen et al. (2004). Sudden collapse would therefore not a viable kinematic model. This would render the hazard and subsequently risk to life negligible. Further analysis is planned to model the slope kinematics and strength over time to test this hypothesis.

References

Braathen, A., Blikra, L. H., Berg, S. S., & Karlsen, F. (2004). Rock-slope failures in Norway; type, geometry, deformation mechanisms and stability. Norwegian Journal of Geology, 84(1), 67-88. ISSN 029-196X.

Frattini, P., Crosta, G. B., Rossini, M., & Allievi, J. (2018). Activity and kinematic behaviour of deep-seated landslides from PS-InSAR displacement rate measurements. Landslides, 15(6), 1053-1070. https://doi.org/10.1007/s10346-017-0940-6

Glastonbury, J., & Fell, R. (2010). Geotechnical characteristics of large rapid rockslides. Canadian Geotechnical Journal, 47(1), 116-132. https://doi.org/10.1139/t09-080

Lauknes, T. R., Grahn, J., Rouyet, L., Larsen, Y., Böhme, M., Dehls, J. F., & Kristiansen, L. (2020). Mapping and characterization of unstable slopes with Sentinel-1 multi-geometry InSAR (activity line 2: public sector applications). https://hdl.handle.net/10037/31490

McColl, S. T., & Draebing, D. (2019). Rock Slope Instability in the Proglacial Zone: State of the Art. In Geomorphology of Proglacial Systems (pp. 119-141). https://doi.org/10.1007/978-3-319-94184-4_8

AN EVIDENCE BASED APPROACH TO QUANTIFYING GEOLOGICAL UNCERTAINTY

LUKE JOHNSTONE
AtkinsRealis, England, Luke.Johnstone@AtkinsRealis.com

Introduction

Geotechnical design relies on an analysis informed by an accurate and reliable representation of ground conditions. Here we will focus on 3D digital geological models used to capture ground conditions and inform design. Typically these are comprised of a series of key geological surfaces built from contacts in ground investigation (GI) data (contacts). At the location of the contacts the surface is considered reliable with a high certainty, however between contacts interpretation is necessary and the surface location is inherently uncertain. Uncertainty increases with distance and the more complex or variable the ground conditions are, the more rapidly the uncertainty increases. It is critical to understand and communicate a surface's reliability and its potential variability in areas between contacts or sparsely populated by GI.

Approaches to uncertainty are discussed in guidance such as IAEG C25 (Parry, et al., 2014) however it is rarely quantified and there is no widely accepted framework for its assessment. As a result, surfaces in ground models are described as best estimates and uncertainty is commented on in accompanying reports and risk registers. As digital deliverables, they may be shared and referenced without the accompanying documents, resulting in design decisions divorced from geological advice.

This paper presents an evidence based geostatistical method to quantify the potential variability in a geological surface (quantified uncertainty) based on the distribution of contacts. Quantified uncertainty is calculated as a function of two factors: distance to GI as defined by the distribution of contacts in the XY dimension and geological complexity as defined by the variability of contacts in the Z dimension (elevation).

It is noted that uncertainty in geological models may arise from a number of factors and that not all geological models are focussed on geological surfaces. This methodology is intended to be used as a tool for robust, transparent, and repeatable design decisions in large infrastructure projects, where large teams of geologists examine and interpret geological data, potentially arriving at differing design decisions.

Method

The methodology calculates variables on a grid across the site, then combines these into a quantified uncertainty. The calculation is undertaken using a Grasshopper script in Rhino. The methodology is described as follows and visualised in Figure 1.

Geological Complexity (C): For each grid cell, the standard deviation (*C)* of nearby contacts elevations is calculated. *C* reflects the variability of the geological surfaces in this area, $2*C$ is taken as the 95th percentile of the potential variability of the geological surface in that area.

Borehole Influence (I): Following a similar methodology to Lelliott et. al. (2009) the GI zone of influence is modelled using a gaussian function centred on the contact location. The standard deviation of the gaussian function is currently assessed by geological judgement however is the focus of future work.

Quantified Uncertainty (U): The quantified uncertainty for each grid cell is calculated using the formula $U = 2*C*I$.

Case Study and Results

The methodology is applied to a Holocene-Pleistocene sedimentary sequence and used as guidance to set design levels for geological surfaces. The sedimentary sequence contains a range of both anthropogenic, erosional and depositional geological surfaces. To assess the effectiveness of the methodology, the GI data was subsampled then applied as input and test data. This application demonstrates the method's effectiveness in quantifying and communicating uncertainty.

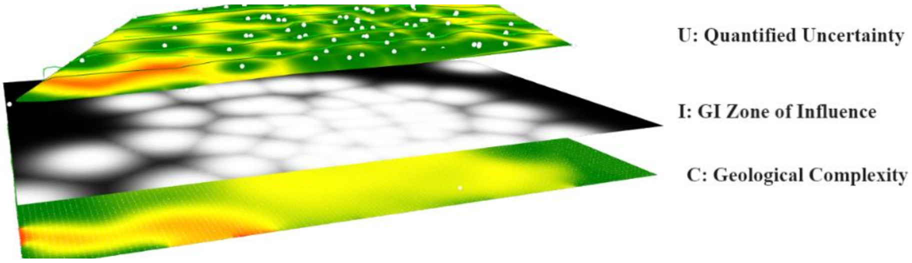

Figure 1. The key compoenents of the methodology visualised as heatmaps

As seen in Figure 1, *C I* and *U* can be displayed as heatmaps, highlighting areas of high risk. The quantified uncertainty can also be displayed as a 95th percentile envelope around a best estimate surface, giving a clear guide on the potential variability of a geological surface (Figure 2).

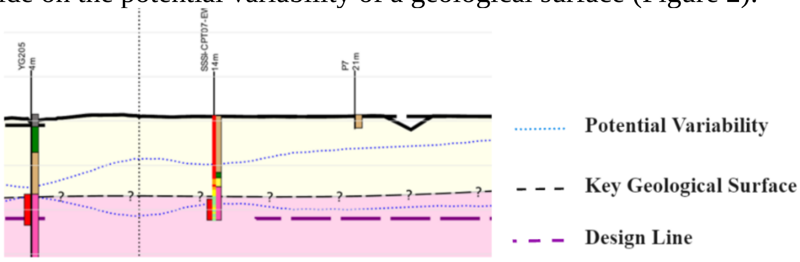

Figure 2. Uncertainty displayed as a 95th percentile envelope

A key weakness of this approach is that it is evidence based and cannot represent hypothesised geological conditions not proven in GI. It is critical that it is used as a decision-making tool paired with a robust conceptual model and geological judgement.

Conclusion

Uncertainty in geological models is a challenging topic often poorly understood and communicated, leading to design decisions disconnected from sound geological judgment. This paper presents a methodology for a systematic, evidence-based approach to quantifying geological complexity. The resulting quantification of uncertainty is clearly communicated, promoting consistent and intelligent design decisions.

References

Fookes, P. (1997). Geology for Engineers: the Geological Model, Prediction and Performance. *Quarterly Journal of Engineering Geology and Hydrogeology*, *30*, 293-424.

Lelliott, M. R., Cave, M. R., & Wealthall, G. P. (2009). A structured approach to the measurement of uncertainty in 3D geological models. *Quarterly Journal of Engineering Geology and Hydrogeology*, 95–105. doi:https://doi.org/10.1144/1470-9236/07-081

Parry, S., Baynes, F., Culshaw, M., Eggers, M., Keaton, J., Lentfer, K., . . . Paul, D. (2014). Engineering geological models: an introduction: IAEG Commission C25. *Bulletin of Engineering Geology and the Environment*, 689. doi:10.1007/s100064-014-0576-x